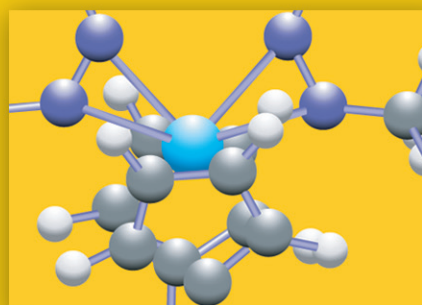
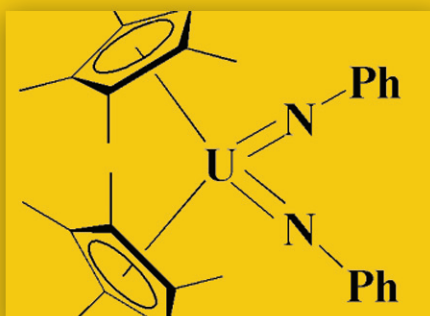


Los Alamos National Laboratory
**ACTINIDE RESEARCH
QUARTERLY**

1st quarter 2004



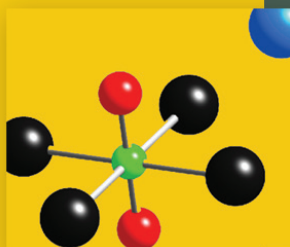
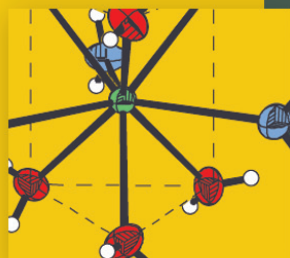
Heavy-Element Chemistry



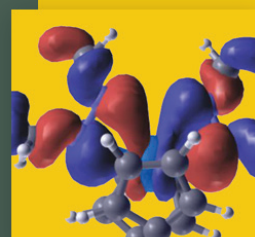
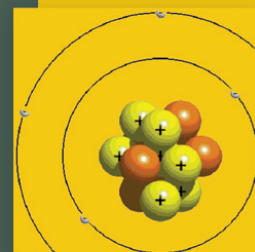
 **Los Alamos**
NATIONAL LABORATORY

CONTENTS

ACTINIDE RESEARCH QUARTERLY



- 1 Heavy-element chemistry at Los Alamos
- 2 Researchers discover fluorescence from a new class of actinyl transitions
- 7 Classic high-symmetry species
- 11 Exploring metal-ligand interactions
- 15 Unusual tetraoxo coordination in heptavalent neptunium
- 20 The correlation between Raman spectroscopy and bond lengths
- 23 Developing a comprehensive picture of the chemical behavior of the 5*f* elements
- 28 Valence orbitals
- 30 Lewis acids and bases
- 31 Electronic structure and bonding in 5*f*-element complexes
- 36 XAFS spectroscopy as a probe of actinide speciation
- 42 Structural characterization of compounds targeted in plutonium separation
- 46 Powder x-ray diffraction
- 47 Single-crystal x-ray diffraction
- 48 Unusual solvent system shows potential to revolutionize technologies
- 52 Russian storage facility commissioned



Heavy-element chemistry at Los Alamos

The chemistry and physics of the actinide elements (uranium, neptunium, plutonium, etc.) have always been of prime importance at Los Alamos, beginning with the early efforts to characterize the chemistry of plutonium during the Manhattan Project. This continuing institutional investment in fundamental actinide science has provided the technical basis for process and separation chemistry and metallurgy related to the national security mission of the Laboratory. As a result, Los Alamos has the expertise, capabilities, and facilities to carry out a wide range of chemical research with the actinide elements, including inorganic, organometallic, and solid-state synthesis; a wide variety of spectroscopic characterization techniques; and modern electronic structure theory.

The actinide series marks the emergence of 5f electrons in the valence shell. In the pure elements, those to the left of plutonium have delocalized (bonding) electrons, while elements to the right of plutonium have localized (nonbonding) electrons. Plutonium is trapped in the middle, and for the delta-phase metal, the electrons seem to be in a unique state of being neither fully delocalized nor localized, which leads to novel electronic interactions and unusual physical and chemical behavior. The concept of localized or delocalized 5f electrons also pervades the bonding descriptions of many of the actinide molecules and compounds. In the normal nomenclature of chemistry, the delocalized electrons are those involved in covalent bonding, while the localized electrons give rise to ionic behavior. Understanding the nature of bonding in actinide materials remains a computational and experimental challenge.

A full understanding of the nature of the chemical bond in actinide systems must access the relative roles of all atomic orbitals in chemical bonding. The articles in this issue of *Actinide Research Quarterly* describe the Los Alamos approach to understanding covalency in actinide molecules and materials. This strategy combines synthetic chemistry, spectroscopic characterization, and theory and modeling to understand and predict the chemical and physical properties of actinide materials. This multidisciplinary approach is the strength of the Los Alamos heavy-element chemistry discipline and provides the scientific means to formulate rational approaches to solve complex actinide problems in a wide variety of environments.

David L. Clark
Gordon D. Jarvinen

The actinide series.

58 Ce	59 Pr	60 Nd	61 Pm	62 Sm	63 Eu	64 Gd	65 Tb	66 Dy	67 Ho	68 Er	69 Tm	70 Yb	71 Lu
90 Th	91 Pa	92 U	93 Np	94 Pu	95 Am	96 Cm	97 Bk	98 Cf	99 Es	100 Fm	101 Md	102 No	103 Lr

Uncharted scientific territory

Researchers discover fluorescence from a new class of actinyl transitions

The fluorescence observed following the interaction of light with actinide oxide species has fascinated people for millennia, in large part because of its visually striking effect.

An artifact of yellow-colored, uranium-doped glass was found near Naples, Italy, and determined to have been made in 79 A.D. Early 19th century European glassmakers added small amounts of uranium to their glass formulations as a coloring agent to make Canary-glass objects in which the appearance is clearly enhanced by the characteristic yellow-green fluorescence. As recently as the late 1930s, uranium oxides were added to the glazes employed to decorate the brilliant red dinnerware developed by Fiestaware. Although the production of uranium glass in the United States was halted in 1942, the marvelous colors of these uranium-containing objets d'art continue to appeal to enthusiasts today.

Intrigue

The historical importance of uranyl fluorescence is not only artistic, but also scientific as well. The Canary-glass objects popular in the 19th century attracted the interest of the Scottish scholar Sir David Brewster, who mentioned the first scientific observation of visually appealing green fluorescence of uranium-containing glass in 1849. The term for this fundamental phenomenon, fluorescence, was later introduced by Sir George Gabriel Stokes in 1852 in his paper titled "The Change in the Refrangibility (wavelength) of Light." In this historic work, he described fluorescence from uranium oxide analytes:

"The intervals between the absorption bands of green uranite were nearly equal to the intervals between the bright bands of which the derived spectrum consisted in the case of yellow uranite. After having seen both systems, I could not fail to be impressed with the conviction of a most intimate connexion [sic] between the causes of the two phenomena, unconnected as at first sight they might appear. The more I examined the compounds of uranium, the more this conviction was strengthened in my mind."

This work contributed to the rule that emitted light is always of longer wavelength than that of the exciting light, a principle that is now called Stokes' Law. In modern years, fluorescence from compounds containing uranyl ions has attracted widespread attention as a tool for understanding the complex electronic structure of actinide molecules, characterizing speciation

Early 19th century European glassmakers added small amounts of uranium to their glass formulations as a coloring agent to make Canary-glass objects. A uranium-glass candy dish is shown before illumination (top left) and after illumination (center left) with ultraviolet light. The Canary-glass Bohemian perfume bottle (bottom left) dates from the mid-19th century. As recently as the 1930s, uranium oxides were added to the glazes used to create the brilliant red color of dinnerware developed by Fiestaware, such as the cup and saucer shown below.

Photos by Mick Greenbank



This article was contributed by Los Alamos researchers Marianne Wilkerson and Harry J. Dewey of the Chemistry Division and John Berg of the Nuclear Materials Technology Division.





Laser-induced fluorescence spectroscopy is used to probe the electronic structure of neptunyl compounds. John Berg collects fluorescence data from a sample containing $Cs_2U(Np)O_2Cl_4$ while Marianne Wilkerson adjusts the sample.

fluorescence from an actinyl species other than uranyl. A team led by Marianne Wilkerson and Harry Dewey of the Chemistry Division and John Berg of the Nuclear Materials Technology Division has established a capability at the Integrated Spectroscopy Laboratory to detect near-infrared photons emitted by actinide compounds following visible laser excitation. The spectra arise from a $5f-5f$ transition, opening up the ability to explore the electronic structure of actinide compounds in the near-infrared region of the electromagnetic spectrum by using sensitive and selective spectroscopic capabilities. This research is part of a Basic Energy Sciences (DOE BES) program to investigate chemical behavior of heavy elements.

Actinide challenges and limitations

Many innate chemical properties of molecules are a consequence of electronic structure, or the manner in which electrons are arranged in orbitals around bonding atoms, and the electronic structures of molecules containing actinide elements are especially intriguing and challenging to understand. The large radii and lack of strongly directional bonding of actinide atoms contribute to a large variety of molecular arrangements. Only actinide-containing molecules can house electrons in the $5f$ group of orbitals, and the large number of orbitals in this $5f$ group can interact with other available molecular orbitals, generating intricate electronic structures. Optical spectroscopy is a powerful tool for probing electronic structures of molecules, but the spectral signatures of

of uranium materials, and detecting the presence of uranium. Although investigations of fluorescence from other actinide species are not as extensive, reports from Russian scientists suggest that fluorescence from neptunium analytes is quite sensitive. However, the molecular composition of their neptunium samples is unknown.

Discovery

Researchers at Los Alamos have discovered the first example of

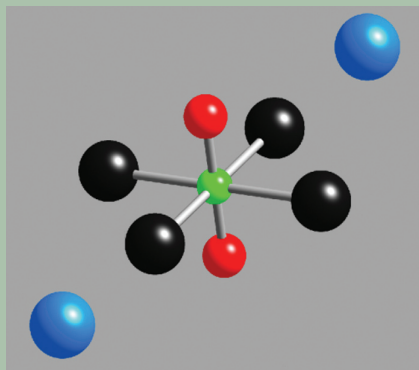
Fluorescence from a sample containing the neptunyl tetrachloride ion can be induced using excitation from a simple helium neon laser source.



The neptunyl tetrachloride ion

The neptunium compound chosen to initiate this fluorescence investigation is $\text{Cs}_2\text{NpO}_2\text{Cl}_4$. The structure of this relatively simple molecule consists of a neptunium atom coordinated in a pseudo-octahedral fashion by two apical oxo groups and four equatorial chloride ligands such that the $\text{NpO}_2\text{Cl}_4^{2-}$ anion is centrosymmetric and has approximate D_{4h} symmetry. The charge of the dianion is balanced by two cesium cations. This class of molecular solids is particularly amenable to fluorescence studies because the preparation of $\text{Cs}_2\text{NpO}_2\text{Cl}_4$ is easily carried out in air, the simple chloride ligands lack any intraligand vibrational modes that could give rise to complicating vibronic structure or fluorescence quenching, and the lack of water in the crystalline lattice eliminates another potential source of fluorescence quenching.

Dilution, or doping, of a fluorescent ion or molecule into a host crystal is often necessary to minimize self-quenching and to offer some degree of control over the local environment. Model host material should have sites of appropriate size for accommodating the dopant, be chemically unreactive with the dopant, and lack any high-frequency vibrational modes that could serve as acceptors for radiationless deactivation. $\text{Cs}_2\text{UO}_2\text{Cl}_4$ is an ideal host for inclusion of $\text{Cs}_2\text{NpO}_2\text{Cl}_4$ because it is isostructural and only slightly larger in size, and its spectroscopic signature offers a large optical window throughout the near-infrared into most of the visible spectrum. Furthermore, there is a fortuitous wealth of supporting information on both $\text{Cs}_2\text{UO}_2\text{Cl}_4$ and $\text{Cs}_2\text{NpO}_2\text{Cl}_4$ obtained from complementary spectroscopic methods.



Researchers used the neptunium compound $\text{Cs}_2\text{NpO}_2\text{Cl}_4$ in their fluorescence investigation. Neptunium is green, oxygen is red, chlorine is black, and cesium is blue.

actinide compounds are complicated due to extensive numbers of spectral lines. As a result, correlations between the molecular structures and optical spectra of actinide molecules remain difficult to predict or even describe.

Opportunities

To date, a large number of the spectroscopic studies of actinide compounds have focused on understanding the electronic structure and optical spectra of uranyl, a ubiquitous anion consisting of a metal that is coordinated by two oxygen ligands in a trans fashion. The electronic spectra of uranyl compounds are characterized by a particular type of interaction in which an electron is excited from an orbital that is mostly associated with the oxygen atoms to an orbital that is more representative of the central metal atom. These so-called ligand-to-metal charge-transfer (LMCT) transitions are readily detected using fluorescence, which in some cases is visible to the unaided eye in the mesmerizing yellow and green colors of uranium oxide compounds.

Efforts toward understanding the electronic structures of all other actinide species, however, are much less common. One complicating factor is that there is an additional class of transitions available to these other species: transitions that correspond to promotion of an electron from one state of predominantly $5f$ metal orbital character to another state of primarily $5f$ metal orbital character. As suggested earlier, the number of possible excitations involving $5f$ electrons complicates theoretical treatment. Furthermore, fluorescence transitions involving electrons in $5f$ orbitals will not be found in the easily detected visible region of the optical spectrum, but rather in the near-infrared region, where detection technology has been much less advanced until recently.



Many spectroscopic studies of actinide compounds have focused on understanding the electronic structure and optical spectra of the uranyl ion, a cation consisting of a metal that is coordinated by two oxygen ligands in a trans fashion. This is the structure of an actinyl ion ($M = \text{uranium, neptunium, plutonium, or americium}$). The electronic spectra of uranyl compounds, which are characterized by so-called ligand-to-metal charge-transfer transitions, are detected using fluorescence, but some of them are visible to the unaided eye, as seen in the yellow and green colors of uranium glass.

The discovery that fluorescence from the neptunyl ion is observable, particularly near-infrared fluorescence, opens uncharted scientific territory for the study of a significant class of transitions available to other stable forms of uranium, neptunium, plutonium, and americium. The signatures mapped out by $5f$ - $5f$ transitions are relatively simpler than those of LMCT transitions with regard to the numbers of electronic states and potential relaxation pathways. The ability to probe these transitions with molecular fluorescence will enrich our understanding of the fundamental properties of $5f$ orbitals, such as their role in actinide bonding, transition probabilities as a function of temperature, and the lifetimes of excited states.

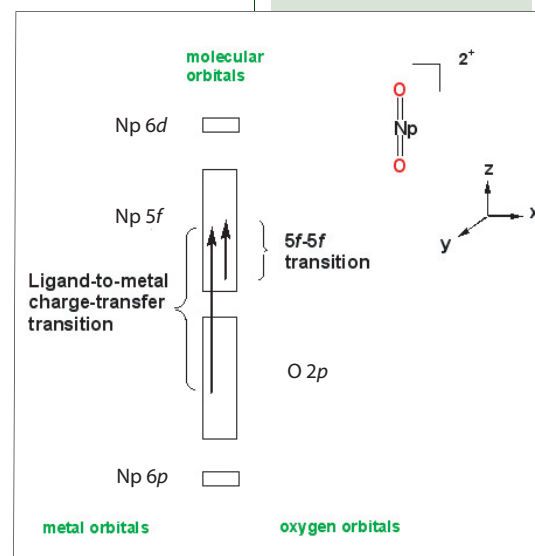
Applications

Researchers are attempting to develop near-infrared fluorescence to complement a variety of other techniques for a Laboratory Directed Research and Development-Directed Research (LDRD-DR) project aimed at a fundamental scientific understanding of the interaction of actinide molecules with oxide minerals within the solid (mineral)/water interface. By coupling these experiments with transport models and other techniques, researchers hope to develop a better understanding of interfacial reactions of actinides in the environment.

Collective results suggest that neptunium fluorescence may have practical application as a detection capability. Russian researchers claimed more than ten years ago that a neptunium detection limit as low as a few picograms could be achieved through fluorescence detection in the red region of the visible spectrum. New data suggests that this region may not be where even the most intense signal should occur.

The Los Alamos team has discovered that the neptunyl ion fluoresces with reasonable efficiency in the near-infrared not only at liquid-nitrogen temperature, but more significantly at room temperature. Furthermore, fluorescence is readily achieved using excitation by red light of a simple helium neon laser or diode lasers common in consumer electronic devices. Specific optical transitions also can be identified by their characteristic energy and by an additional identifying tag, the length of time that an electron resides in an excited state before the excitation decays in a fluorescence transition. Measurements by Los Alamos researchers reveal that low-lying excited states of neptunyl may have reasonably long lifetimes, comparable to those of uranyl species.

Understanding the electronic structures of actinide species other than uranyl is complicated by the fact that there is an additional class of transitions—the $5f$ - $5f$ transition—available to these other species. In this type of transition, an electron is promoted from one state of predominantly $5f$ metal orbital character to another state of primarily $5f$ metal orbital character. This figure shows the transitions available to the neptunyl ion.

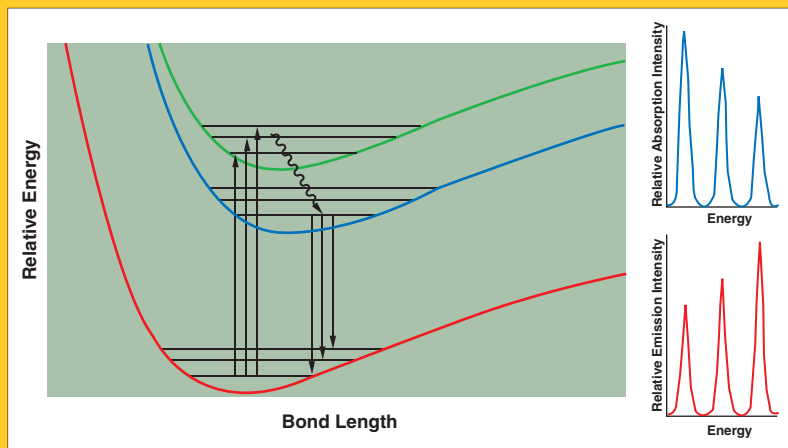


How does a molecule interact with a photon of light?

Every molecule has a characteristic set of electronic states, each of which is defined by a particular arrangement of the molecule's electrons into molecular orbitals. These electronic states lie at different energies. Most of the time a molecule resides in the state of the lowest energy, known as its ground state, but there are accessible higher-energy states known as excited states. One way that a molecule may be transformed into an excited state is by absorbing a photon of light whose energy matches the difference in energy between the ground state and an excited state of the molecule. When this absorption occurs, the electrons rearrange to form the excited state. A plot of the tendency to absorb light versus the photon energy is known as an absorption spectrum and exhibits peaks that correspond to energy differences between the ground and excited states.

Because a molecule is inherently unstable in an excited state, it tends to return to the ground state by any of several pathways. The length of time that the molecule resides in an excited state before it decays to a lower-energy state is termed the excited state lifetime. One of the decay pathways is by emission of a photon in a process known as luminescence, a word coined from the Latin word for light—lumen. Luminescence is a relatively rare decay pathway for excited states of most molecules, but if it occurs, it greatly eases the detection and study of excited states, making its discovery in a neptunium-containing molecule particularly interesting.

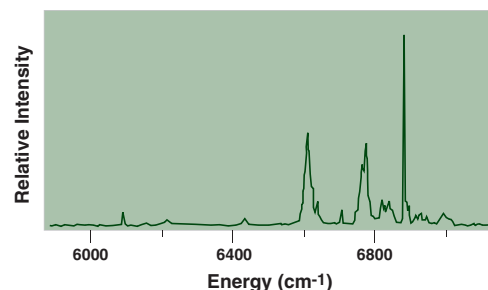
The characteristic vibrations of the molecule may also be excited by either absorption or luminescent processes. Much of the complex structure in an absorption spectrum is due to excitation of one or more quanta of vibrational energy in addition to the change of electronic states.



The absorption versus luminescent process is defined in this illustration. The red curve represents the potential energy of a lower-lying electronic state such as the ground state and the blue curve represents the potential energy of an excited electronic state. The black levels on each curve symbolize the energy of levels of a vibrational mode. When an absorption process occurs, a photon of appropriate energy is absorbed by a molecule, promoting the molecule to a vibrational level of a higher-lying electronic state. Conversely, when a luminescent process occurs, a photon is emitted by a molecule in an excited state, allowing it to relax to a vibrational level of a lower-lying state.

Future

It had been presumed that fluorescence, the workhorse technique for understanding uranyl LMCT transitions, was unemployable for observing the $5f$ excitations that are much more common in all other dioxo actinide species. The team's discovery of $5f$ - $5f$ fluorescence from the neptunyl ion has revealed a new and exciting tool for future fundamental studies of electronic structure and applied development of detection technologies.



Recent advances in detection technology have made it possible to observe fluorescence transitions in the near-infrared region, as shown in this fluorescence spectrum of $\text{Cs}_2\text{NpO}_2\text{Cl}_4$, the compound used by Los Alamos researchers in the early part of their investigation.

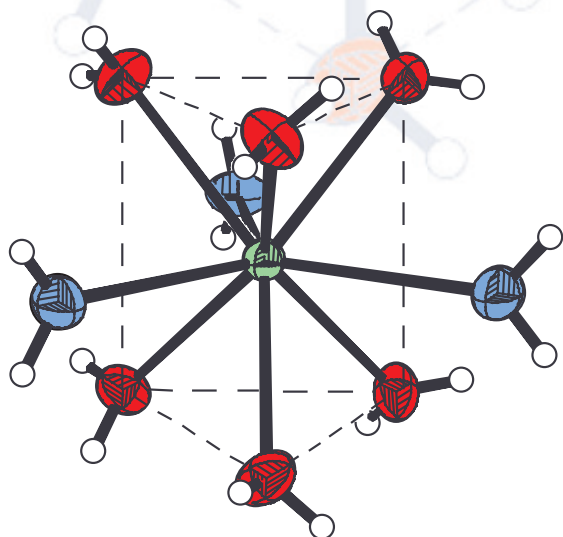
Homoleptic nine-coordinate An(III) and Ln(III) complexes
Classic high-symmetry species that advance our understanding of *f*-element structure, bonding, and dynamics

Understanding the behavior of actinide and lanthanide ions in water and other solvent media remains one of the great experimental and theoretical challenges in *f*-element chemistry. The behavior of actinide ions in aqueous solution is highly relevant to issues in nuclear material processing, concerns about actinide-ion transport in groundwater, and hydrological implications of spent fuel storage strategies. The strong Lewis acidity of the actinide ions leads to complex, highly pH-dependent equilibria in aqueous media. (Lewis acids are substances with a strong affinity for accepting electron pairs, but which do not necessarily directly affect hydrogen ion concentration).

Understanding the nature of *f*-element-solvent interactions is also important for fuel cycle processes such as actinide/lanthanide separations and require an understanding of the intimate coordination sphere of solvent molecules about actinide and lanthanide ions, of the interactions of the primary coordination complexes with the bulk solvent that surround them, and of the dynamical processes between the coordinated and bulk solvent molecules.

Successful modeling of the behavior of lanthanide and actinide ions in solution begins with a detailed understanding of the direct interactions between the ions and solvent molecules as ligands. The level of understanding necessary for such modeling can greatly benefit from studying the bonding, electronic structure, spectroscopy, and chemical properties of well-defined coordination complexes of the early actinides. Given the importance of isolating the important ion-solvent interaction, the strategy of using noncoordinating or very weakly coordinating counterions was adopted; exemplary is the trifluoromethane sulfonate anion (CF_3SO_3^- , commonly called triflate).

Triflate salts of Pu(III) and Am(III) aquo complexes— $[\text{An}(\text{OH}_2)_9][\text{OTf}]_3$ —were prepared, in which the oxygen atoms of the nine-coordinated water molecules adopt a highly symmetric tricapped, trigonal-prismatic (TCTP) geometry about the Pu^{3+} and Am^{3+} ions. Lanthanide triflates having the same compositions and analogous geometries are well characterized, allowing for a direct comparison between the structure and bonding in An(III) and Ln(III) complexes.



This thermal ellipsoid representation shows the ideal tricapped, trigonal-prismatic structure of the Pu(III) aquo complex (the triflate anion is not shown). The six symmetry-equivalent prismatic oxygen ligands (red) define the vertices of the trigonal prism. The three capping oxygen ligands (blue) are positioned outside the rectangular faces of the prism. The plutonium atom (green) is in the center.

This article was contributed by Los Alamos researcher Mary P. Neu of the Chemistry Division and Jason L. Sonnenberg and Bruce E. Bursten of the Department of Chemistry, The Ohio State University.

HIGH-SYMMETRY SPECIES

Theoretical studies have shown that the vacant 6d atomic orbitals of the actinide atom (in this case plutonium) are the principal sites of ligand electron acceptance. This contour plot of $\text{Pu}(\text{H}_2\text{O})_9^{3+}$ shows the water ligands donating primarily into the plutonium 6d orbitals.

Because the valence electronic structure of actinide ions are dominated by atomic 5f and 6d orbitals, whereas that of the lanthanide ions involves the 4f and 5d orbitals, the comparison of these two classes of complexes might provide valuable insight into how electronic structure affects geometric structure and reactivity.

The TCTP structure has six symmetry-equivalent prismatic ligands at the vertices of a trigonal prism. The remaining three ligands are capping ligands positioned outside the rectangular faces of the trigonal prism. The capping ligands are equivalent to one another by symmetry, but are unique from the six prismatic ligands. As such, the metal-ligand distances for prismatic and capping ligands can be different as demonstrated in the Pu(III) aquo structure, which contains Pu-OH₂ bond distances of 2.574(3) Å for the capping waters and 2.476(2) Å for the prismatic waters. Bond distances for the Am(III) complex are slightly shorter, correlating well with the decrease in ionic radius across the actinide series.

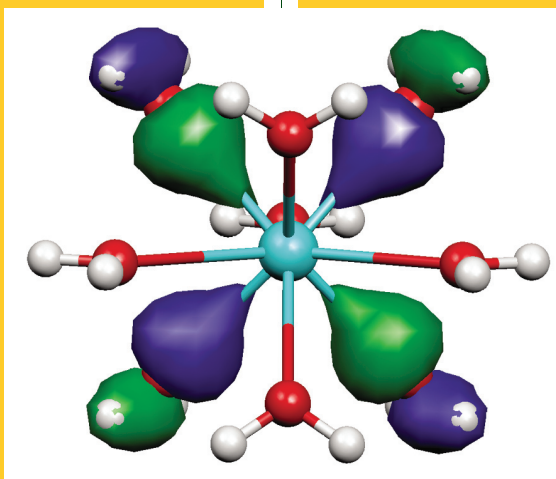
We are engaged in computational modelling of these actinide species in solution. Our theoretical studies of solvated *f*-element ions (those chemically bound to solvent molecules such as water) will ultimately use a combination of quantum mechanics and molecular dynamics. The electronic structural description of the direct interactions of the solvent molecules with the *f*-element

ions requires relativistic quantum chemical techniques.

Once the primary coordination sphere (first layer of solvent molecules surrounding the central dissolved ion) is correctly described, molecular dynamics will be used to model the interaction of the first-coordination-sphere complex with the bulk solvent. The crystalline experimental complexes, which isolate the first coordination sphere, thus provide an opportunity to test the quantum chemical description of the

metal-ligand interactions. In the present studies, density functional theory (DFT) has been used to perform this assessment. Scalar relativistic effects were included via the zero-order regular approximation (ZORA) method.

The structure of isolated $\text{Pu}(\text{H}_2\text{O})_9^{3+}$ was calculated using relativistic DFT with the ion constrained



to a rigorous TCTP geometry. These calculations will suffice for discussing the σ donation from the H₂O ligands into appropriate acceptor orbitals on the plutonium center. The calculated Pu-O bond distances ($\text{Pu-O}_{\text{cap}} = 2.619 \text{ \AA}$ and $\text{Pu-O}_{\text{pris}} = 2.540 \text{ \AA}$) are slightly longer than those observed in the crystal structure. Interactions involving the second lone pair of each H₂O ligand will involve subtle Pu-O π effects. π bonding describes a particular type of overlap between the atomic orbitals of bonding electrons, differing from the more symmetric σ electron-density overlap.

It is important to note that the calculations predict correctly that the Pu–O_{cap} distance is longer than the Pu–O_{pris} distance. Relaxing the symmetry to allow the water molecules greater rotational freedom, which will allow them to maximize their π bonding to the Pu³⁺ center, could lead to some shortening of the Pu–O bonds and improve the agreement with the observed crystal structure. Overall, there is clearly good agreement between experiment and theory on these complex systems under the constraints of high symmetry and without specific consideration of anion effects.

The calculations on Pu(H₂O)₉³⁺ provide insights into the nature of the Pu–OH₂ bonding. As expected, the water ligands act as electron-pair donors (Lewis bases) that donate electron density to the Pu³⁺ ion, which serves as an electron acceptor (Lewis acid). Our previous theoretical studies of organo-actinide complexes demonstrated that the vacant *6d* atomic orbitals of the actinide atom served as the principal sites of ligand electron acceptance, whereas the *5f* orbitals were used to house any metal-based electrons. The same bonding paradigms appear to be present in Pu(H₂O)₉³⁺. The water ligands donate primarily into the plutonium *6d* orbitals.

Because a neutral plutonium atom has eight valence electrons, the Pu³⁺ ion is expected to have five metal-based electrons. Our research indicates that this is indeed the case and that those electrons reside in nearly pure plutonium *5f* orbitals. This dichotomy in the roles of the actinide *5f* and *6d* orbitals will change somewhat for lanthanide complexes because of the

different spatial extents of the atomic orbitals between the two rows of the periodic table.

From experimental studies, we can compare the plutonium and americium aquo structures with those for lanthanides of similar ionic radii, Nd(III) and Sm(III). The capping waters have nearly identical bond

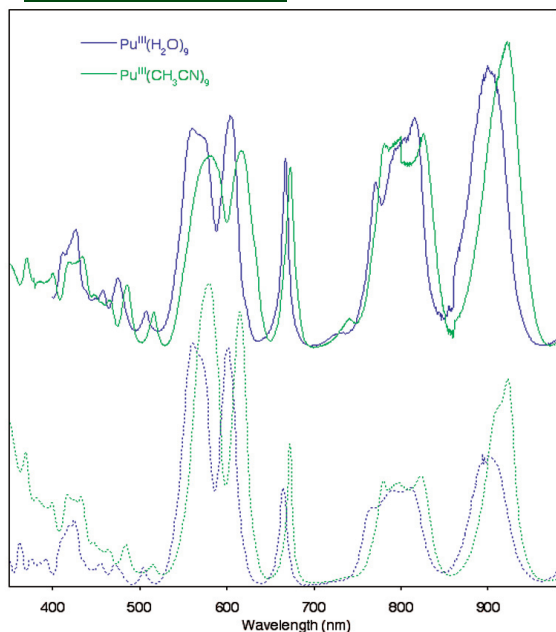


lengths, while the An(III) prismatic waters are approximately 0.03 Å shorter than those of the Ln(III) with the same ionic radii. Electronic structure calculations aimed at explaining these differences are under way.

To further explore the structure and bonding properties, we have recently prepared nonaqueous trivalent actinide complexes that are nearly isostructural with the aquo complexes and contain weaker σ -donor ligands coordinated to the metal. For example, [Pu(NCMe)₉][PF₆]₃·MeCN was prepared by treating an acetonitrile suspension of Pu-239 metal turnings under argon atmosphere with three equivalents of either AgPF₆ or TlPF₆. Compared with the Pu–O in the aquo complex, the average Pu–N distance (2.572 Å) is 0.047 Å longer. The geometry of the acetonitrile complex is distorted rather than ideal TCTP, perhaps because the PF₆[−] ion is more strongly coordinating than the triflate anion.

To study structure and bonding properties of actinides, researchers dissolve Pu-239 metal strips (shown in the vial above left) or metal powder in water or acetonitrile and place them under an argon atmosphere. The resulting solids (shown in the photo at right and in this case plutonium strips dissolved in acetonitrile) are analyzed by a number of methods, including single-crystal x-ray diffraction.

HIGH-SYMMETRY SPECIES



Optical absorbance and diffuse reflectance spectra suggest that Pu^{3+} has very similar coordination geometries in the solution and solid states of the acetonitrile and aquo complexes. This in turn suggests that the ion is nine-coordinate in solid and solution forms and in both solvent environments. The acetonitrile spectra are shifted by about 15 nm relative to the aquo spectra, reflecting the differing Lewis basicity of the ligands. The top two spectra are diffuse reflectance spectra of the solids. The bottom two spectra are the absorbance spectra of the solutions.

0.025 Å difference in the atomic radii of U and Pu. The three 2.65 Å capping U–N interactions in the U complex are longer than the prismatic interactions by 0.05 Å, and 0.087 Å longer than the average Pu–N capping interactions in the plutonium acetonitrile complex. This U–N capping distance is 0.062 Å longer than that predicted by atomic radii differences between U(III) and Pu(III).

Diffuse reflectance spectra obtained on ground crystals of the solids and optical absorbance spectra of the solutions for the aquo and acetonitrile complexes are nearly superimposable, but each feature in the spectrum of the acetonitrile complex is red-shifted by approximately 15 nm, providing spectroscopic evidence of the difference in bond strengths.

In contrast to the plutonium complex, the uranium acetonitrile adduct we prepared displays nearly ideal TCTP geometry. The six prismatic U–N distances are 2.60 Å. The difference between the average prismatic M–N distances of Pu and U complexes is 0.026 Å, which is close to the

Compared to nine-coordinate acetonitrile Ln(III) tricapped trigonal prismatic adducts (Ln = La, Sm, and Pr), the three capping Ln–N distances are on average slightly shorter than the six prismatic ones in the crystal structures of La ($\Delta_{\text{avg}} = 0.016$ Å) and Pr ($\Delta_{\text{avg}} = 0.004$ Å). This trend reverses in the Sm complex ($\Delta_{\text{avg}} = 0.008$ Å). However, the difference between the average prismatic and average capping distance in a particular Ln(NCMe)₉³⁺ compound is small.

Published DFT calculations of the nine-coordinate acetonitrile Ln³⁺ (Ln = Eu, Yb, and La) solvates predicted that the three capping distances of Ln(NCMe)₉³⁺ would be longer than the six prismatic distances. Qualitatively, the uranium complex follows the trend predicted by DFT, but the plutonium complex follows the trend of the experimentally determined lanthanide structures.

We will continue to combine experimental and theoretical methods to explore the rich chemistry of *f*-element complexes in solution. Such judicious combination of synthetic and structural chemistry with modern computational modelling provides understanding of a very complex and relevant topic in current *f*-element chemistry.

This research is supported by the DOE Office of Basic Energy Sciences.

Capability complements experimental probes

Exploring metal-ligand interactions in actinide complexes using density functional calculations

Modern quantum chemistry techniques can provide insights into electronic properties of actinide complexes such as the nature of the chemical bonding, the structures and relative energies of related compounds, and the nature of electronic excited states. The results are obtained from quantum mechanical calculations that treat the interactions of the electrons with the nuclei in the molecule. From the solution of the molecular Schrödinger equation, wave functions can be obtained that describe the electrons, and, in turn, the overall electronic density in the molecule.

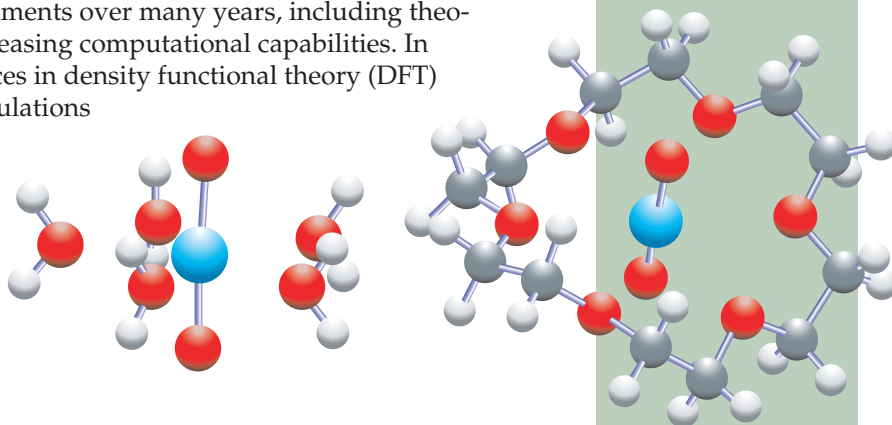
The ability to perform reliable calculations on actinide species is a result of several developments over many years, including theoretical methods and increasing computational capabilities. In particular, recent advances in density functional theory (DFT) have made possible calculations on large chemical systems compared to conventional quantum chemistry approaches.

Another development involves techniques to treat just the valence electrons (those in the outermost “shells” of atoms that are most likely to participate in the formation of chemical bonds) in molecules containing heavy elements such as actinides. In addition, these approaches simultaneously incorporate the effects of relativity on the valence electrons, since relativistic effects are crucial in this region of the periodic table.

Oxo complexes as testbeds

Among the most prevalent motifs in the chemistry of higher-valent actinide species are actinyl species comprised of a linear bonding linkage $[O=U=O]^{2+}$ as in the uranyl (UO_2^{2+}) species that generally coordinates to other molecules (ligands) by forming bonds around a central plane about the UO_2^{2+} unit. Typical examples are the aquo complex $[UO_2(H_2O)_5]^{2+}$ and its Np and Pu counterparts that represent the dominant species found in aqueous solution at low pH for the +5 and +6 oxidation states of the actinides. Recent calculations have examined how the molecular structures and calculated vibrational frequencies of the $O=An=O^{2+}$ unit systematically vary across the actinides from U to Np to Pu.

Calculated structures for $[UO_2(H_2O)_5]^{2+}$ (left) and $[(NpO_2)(crown)]^+$ (right) complexes from density functional theory calculations are shown at right. The figure on the left is a typical example of an actinyl species comprised of a linear bonding linkage (the central O–U–O molecule) that is coordinated with five molecules of water bound to the actinide atom in the central plane (U=blue, O=red, and H=white). The figure on the right shows a recently identified organic ligand known as a crown ether—the structure encircling the neptunium molecule (Np=blue, O=red, C=grey, and H=white).



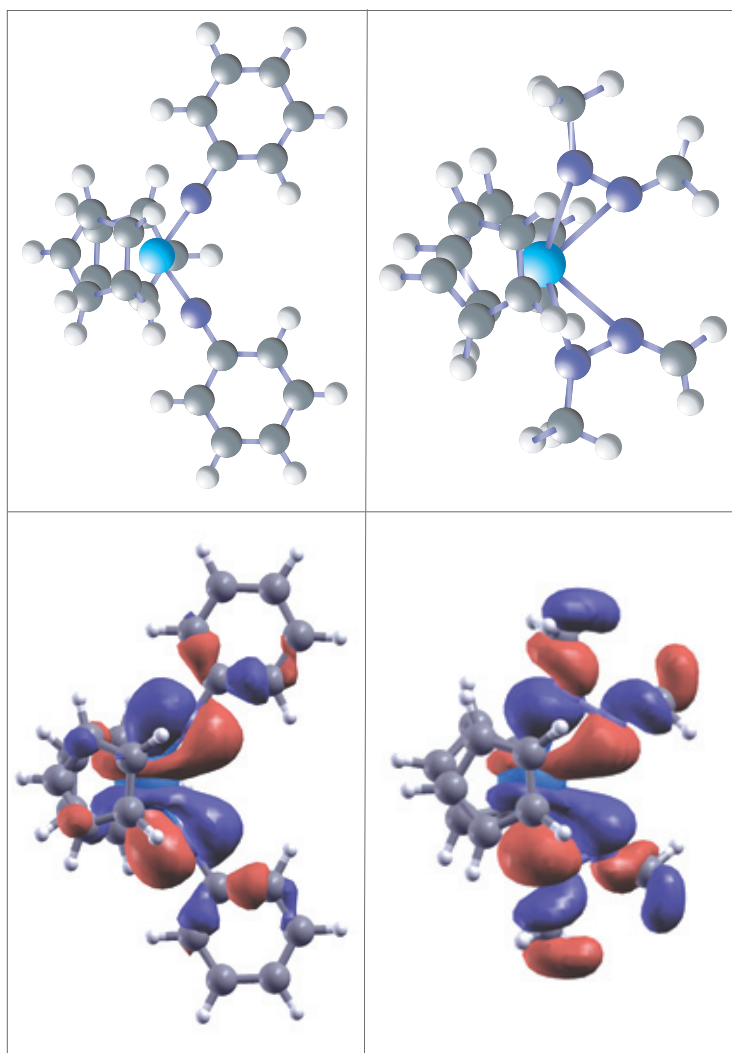
$[UO_2(H_2O)_5]^{2+}$

$[(NpO_2)(crown-6)]^+$

This article was contributed by Los Alamos researchers P. Jeffrey Hay and Richard L. Martin of the Theoretical Division.

METAL-LIGAND INTERACTIONS

These two organoactinide species illustrate the role density functional theory plays in understanding bonding in the actinides. The top left figure is the calculated structure of the U(VI) complex $Cp^*_2U(NPh)_2$, which has no unpaired electrons. The top right figure is the calculated structure of the U(IV) complex $Cp^*_2U(CH_3-N-N-CR_2)_2$, which has two unpaired 5f electrons. The lower left figure is a contour plot of one of the valence orbitals in $Cp^*_2U(NPh)_2$. The lower right figure is a contour plot of a similar orbital in $Cp^*_2U(CH_3-N-N-CR_2)_2$. The blue and red indicate positive and negative contours, respectively. The larger amount of participation by the U atom in the bonding for the complex on the left is indicated by the relatively larger proportion of contours on the metal relative to the N-containing ligands. By contrast, for the complex on the right, a larger proportion of the contours is found on the N-containing ligands.



These predictions can be compared with data from experimental probes in solution such as XAFS and Raman spectroscopy. Both theory and experiment give the same values for the axial An=O bond length in this series in going from U (1.76 Å) to Np (1.75 Å) to Pu (1.74 Å). The calculated Raman frequencies of the O=An=O²⁺ unit are decreasing from 908–805 cm⁻¹, which may be compared with the observed experimental range of 872–835 cm⁻¹ across the same series. The calculated bond length between the actinide and the equatorial oxygen atoms (2.52 Å) is somewhat

longer than observed by XAFS (2.42 Å).

In addition, solvent effects, which are crucial for predicting reaction energies in solution, can be included by an effective medium model that includes a polarizable dielectric medium surrounding the molecule (for example, water or an aqueous solution of sodium chloride).

One of the challenges in environmental chemistry of actinides has been to characterize and selectively remove such species from waste streams, in chemical processing, or in geochemical formations. Our synthetic chemistry colleagues at Los Alamos recently identified an organic ligand known as a crown ether that binds to the Np(V) oxidation state of neptunyl to form a [(NpO₂)(crown)]⁺ complex. (See ARQ 3rd quarter 1998.)

The calculated structure from density functional calculations is in good agreement with the crystal structure obtained experimentally. The

calculations give a good prediction of the Raman frequency for the O=Np=O vibration (776 cm⁻¹ calculated, 780 cm⁻¹ experimental), the predicted Np–O bond length (1.81 Å calculated, 1.80 Å experimental), as well as other structural features.

The only other analogous compound synthesized to date contains the UO₂²⁺ group. Calculations have been performed for the entire series of complexes for both +5 and +6 oxidation states of U, Np, and Pu for the [AnO₂(crown)]^{q+} species. For most cases the calculations represent predictions where

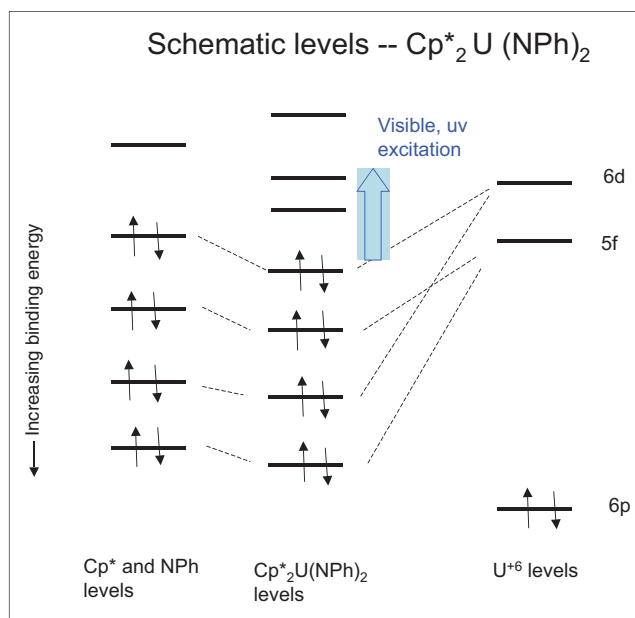
experimental species have not been isolated to date. This illustrates how theory can complement experimental probes to help identify and characterize actinide species of potential environmental interest that may be difficult to isolate or study experimentally.

Understanding bonding and reactivity

Among the novel features of actinide chemistry is the ability of these complexes to involve both $5f$ and $6d$ orbitals in forming chemical bonds. In the actinide series, proceeding across the periodic table entails formally filling up the $5f$ shell. The neighboring $6d$ shell is also energetically accessible, and this shell even lies lower in energy than the $5f$ shell in the early actinides. The principal means by which theory can provide an understanding of the bonding in this actinide series comes from examination of the molecular orbitals. These are the one-electron wave functions for individual electrons in the molecule in the DFT calculations, from which the total electron density for the molecule ultimately is obtained.

Two representative organoactinide species illustrate the role of theory: the bis(imido) U(VI) complex $\text{Cp}^*_2\text{U}(\text{NPh})_2$ and the bis(hydrazonato) U(IV) complex $\text{Cp}^*_2\text{U}(\text{CH}_3\text{-N-N-CR}_2)_2$. In the calculations, a Cp group (C_5H_5) was used to model the permethyl cyclopentadienyl group, C_5Me_5 (Cp^*) as shown in the figure. For more information on the synthesis of these compounds, see the article on page 23. The U(VI) complex has no unpaired electrons, while the U(IV) complex has two unpaired $5f$ electrons. The molecular orbitals describing the other valence electrons can be viewed as arising primarily from the ligands bound to the uranium with some participation by the uranium orbitals. DFT calculations have been performed on both complexes to

examine the nature of the bonding, geometrical structure, and thermochemistry of these complexes. It is often useful to examine the spatial nature and relative energies of the molecular orbitals to understand chemical bonding as well as to explain electronic spectroscopy. In the $\text{Cp}^*_2\text{U}(\text{NPh})_2$ complex, the energy levels of the ligands themselves are stabilized by interactions with both $6d$ and $5f$ orbitals from the U. The energy levels correspond physically to the binding energy needed to remove or excite an electron at a particular energy, since in quantum theory, the molecular energy levels have discrete values.



In visible and ultraviolet spectroscopy, the incident light excites an electron from a filled to an unfilled level as indicated by the arrow. In photoelectron spectroscopy, higher energy x-ray sources are used to ionize the molecule by completely ejecting an electron from the different energy levels.

*This schematic diagram of $\text{Cp}^*_2\text{U}(\text{NPh})_2$ shows the interaction of ligand orbitals (on the left) with $6d$ and $5f$ orbitals of U (on the right) to form the molecular orbitals in the U complex (in the middle). The vertical scale corresponds to the energy needed to remove an electron from a particular filled orbital (electrons are indicated by arrows) and excite it to an empty orbital, as occurs when the molecule absorbs energy in the visible or UV region of the spectrum.*

METAL-LIGAND
INTERACTIONS

If the ligands had their formal charge (such as -1 for Cp*, -1 for hydrazonato and -2 for imido) the U atom in turn would have $+6$ and $+4$ charges associated with its formal valence in the two molecules. The calculations show this ionic picture to be too extreme, since the DFT results give significantly reduced charges on the uranium of only $+1.0$ and $+1.3$ for the U(VI) and U(IV) complexes, respectively.

When all of the bonding electrons are included, this analysis also shows a net “population” of 2.2 $6d$ electrons and 2.5 $5f$ electrons for the U(VI) complex compared to 1.6 $6d$ electrons and 0.8 $5f$ electrons for the U(IV) complex, to which must be added the two nonbonding $5f$ electrons for a total 2.8 $5f$ -electron population.

A large portion of the metal’s participation in the bonding can be traced to a few key orbitals in each system. Two representative orbitals that are qualitatively similar looking are shown in the panels in the figure on page 12. The orbital on the left in the bis(imido) complex has substantial U $5f$ involvement (35% $5f$ of the overall orbital containing a pair of electrons) compared to only 11% $5f$ involvement in the bis(hydrazonato) complex. This translates into greater covalent bonding interactions (in fact multiple-bonding character) in the bis(imido) complex.

While these aspects are beyond the scope of this discussion, it is informative to consider the electronic spectroscopy of these molecules in terms of excitations from these bonding orbitals to unfilled orbitals. If the unfilled orbitals correspond to $5f$ or $6d$ metal orbitals, they would be denoted as charge-transfer excitations compared to ligand-based excitations if both pairs of orbitals reside on the ligand. In addition, as in the case of the U(IV) complex with a $5f^2$ configuration, there are also low-lying excitations arising from filled to unfilled $5f$ excitations that give rise to the absorption spectra in the visible and near-IR region. Finally, the energies and orbital makeup of the occupied levels can be used to compare with photoelectron spectra that probe the molecular binding energies.

These examples serve to show how DFT electronic structure calculations can be used to calculate molecular structure and spectroscopic properties of actinide complexes. The close agreement between theory and experiment for known compounds gives us reasonable confidence in our ability to use DFT theory to predict properties of compounds that have not yet been prepared and provides valuable insight and guidance for interpreting the nature of covalency and chemical bonding and interpretation of spectroscopic properties.

The research on aqueous complexes was supported by a Laboratory Directed Research and Development (LDRD) project administered by the Glenn T. Seaborg Institute at Los Alamos National Laboratory. The organoactinide research is supported by the DOE Office of Basic Energy Sciences.

A unique role for 5f orbitals in bonding

Unusual tetraoxo coordination in heptavalent neptunium

The light actinide elements—uranium, neptunium, plutonium, americium, and curium—in their highest oxidation states (V–VII) have an unusually high affinity for formation of metal-oxygen bonds and demonstrate a high degree of covalency and metal-ligand multiple bonding. This is particularly true for oxo complexes, where, for example, the U=O multiple bond in the UO_2^{2+} ion is remarkably short, and the mean bond strength is similar to that of the C=O bond in CO_2 .

These unusually strong bonds can be traced to the ability of the uranium atom to use a combination of 5f, 6d, and 6p atomic orbitals in chemical bonding. Understanding the relative roles of the actinide 5f, 6d, and 6p atomic orbitals in forming such strong bonds has been a fundamental challenge in actinide chemistry since the recognition of the presence of the 5f series, and a good deal of the fundamental chemistry and physics of light actinides has been devoted to understanding the nature of these bonding interactions.

Historically, the relative roles of 5f/6d/6p atomic orbitals in forming chemical bonds within the linear dioxo ion (AnO_2^{2+}) of hexavalent actinides generated a healthy scientific debate. Much of this debate originated at Los Alamos, as exemplified by the seminal arguments on why ThO_2 is bent in the gas phase and UO_2^{2+} is always linear. It took the clever application of two-photon spectroscopy and oxygen k-edge x-ray absorption spectroscopy by Robert Denning of Oxford University to sort it all out.

What we learned from those studies has changed our fundamental thinking about valence orbitals in heavy-element chemistry. The radial distributions of the early actinide 6s and 6p atomic orbitals are not buried within the core of the atom but lie in the valence region

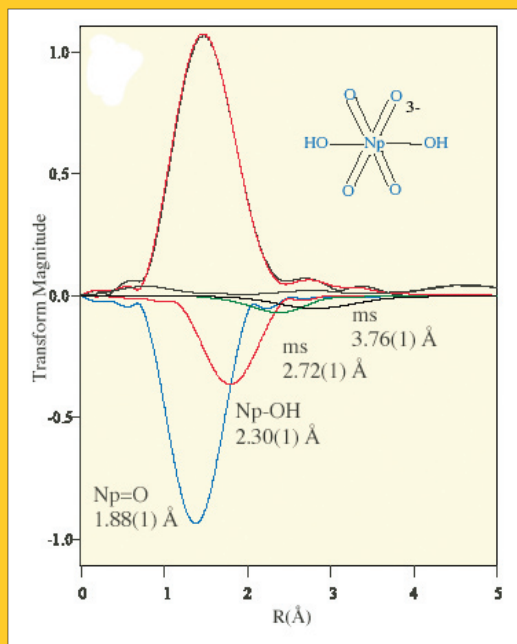
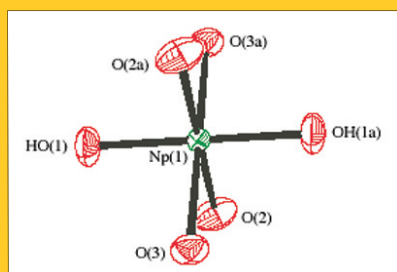
and must be considered to be active in chemical bonding. The ability of the 6p orbitals to hybridize with the 5f can lead to unusually strong σ bonding, and this type of 6p-5f hybridization was shown to be a predominant contributor to the strong covalent bonds in linear UO_2^{2+} ions.

More recently, we have turned our attention to light actinide ions in even higher oxidation states to look for evidence of increased covalency and 5f orbital participation in bonding. Our early studies have focused on developing the basic understanding of the molecular structure of actinide ions in the heptavalent state (oxidation state VII) based on x-ray diffraction and absorption, and assessing the relative bond strengths as determined by nuclear magnetic resonance and vibrational spectroscopy.

This article was contributed by Los Alamos researchers David L. Clark of the Nuclear Materials Technology Division; Phillip D. Palmer, C. Drew Tai, and D. Webster Keogh of the Chemistry Division; Steven D. Conradson, of the Materials Science and Technology Division; and Robert J. Donohoe of the Biosciences Division.

The remarkable strength of actinide-oxygen bonds: a comparison of gas-phase bond enthalpies

UO_2	710 kJ/mole
UO_2^{2+}	701 kJ/mole
MoO_2	587 kJ/mole
CO_2	802 kJ/mole

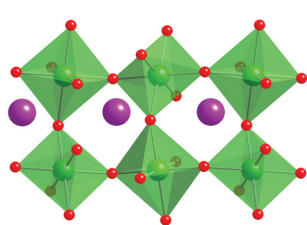


Molecular structure determination of the $\text{NpO}_4(\text{OH})_2^{3-}$ ion

The molecular structure of the $\text{NpO}_4(\text{OH})_2^{3-}$ ion (top) in the solid state was determined by x-ray crystallography. This thermal ellipsoid drawing emphasizes the pseudo-octahedral coordination geometry about the central neptunium ion.

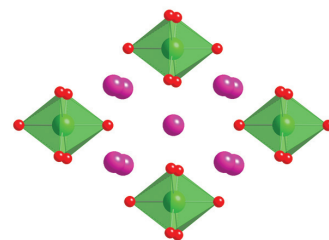
This ion has four short Np-O bonds (1.88 \AA) perpendicular to the page and two long Np-OH bonds (2.33 \AA) in the plane of the page. The structural parameters for the $\text{NpO}_4(\text{OH})_2^{3-}$ ion (bottom) were also determined by XAFS spectroscopy. This figure shows the Fourier transform of the XAFS spectrum (solid black line) and the theoretical fit (dashed red line). The components of the fit, shown beneath the spectrum with negative amplitudes, correspond to individual shells of atoms. Note that there are no atoms at 2.72 and 3.76 \AA . The peaks labeled "ms," which are routinely observed in XAFS data of linear ions, are due to multiple scattering of a photoelectron off the oxygen atoms in the linear O=Np=O unit. The radii of the coordination shells observed in the XAFS (1.88 and 2.30 \AA) match the solid-state structure, giving high confidence that the $\text{NpO}_4(\text{OH})_2^{3-}$ anion is present in solution.

The heptavalent oxidation state of actinide ions is rare, but has been known since the late 1960s due largely to the pioneering efforts of Russian scientists V.I. Spitsyn and N.N. Krot. X-ray diffraction data show that heptavalent neptunium can exist in the familiar trans dioxo form, as illustrated by the structure of CsNpO_4 shown in I, or in an unusual tetraoxo form with a square planar arrangement of O atoms, as indicated by the structure of Li_5NpO_6 shown in II, though we note that the identity of this structure has been recently questioned by L.R. Morss and coworkers at Argonne National Laboratory.



I

Solid-state structure of CsNpO_4 . This structure has a pucker layer of NpO_4 sheets, with axial Np=O bonds above and below the layer. Np atoms are green, O atoms are red, and Cs atoms are purple.



II

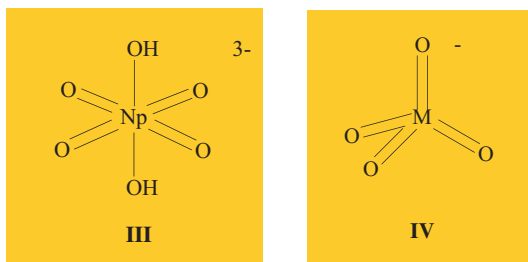
Solid-state structure of Li_5NpO_6 . This structure has an isolated unit, with four equatorial Np=O bonds above and below the plane of metal atoms, and two short Np-O bonds within the plane. Np atoms are green, O atoms are red, and Li atoms are purple.

To understand the nature of chemical bonding in the unusual square planar tetraoxo ion, we have been studying the physical and spectroscopic properties of discrete molecular forms of heptavalent neptunium and plutonium. For example, we have determined the molecular structure of the discrete $\text{NpO}_4(\text{OH})_2^{3-}$ ion by x-ray diffraction in the solid state and by XAFS spectroscopy in both the solid state and solution. Using a technique pioneered by Krot and coworkers at Moscow's Institute of Physical Chemistry, we isolated the $\text{NpO}_4(\text{OH})_2^{3-}$ ion from alkaline solution, using a rather large $\text{Co}(\text{NH}_3)_6^{3+}$ cation, to give a solid compound of formula $[\text{Co}(\text{NH}_3)_6][\text{NpO}_4(\text{OH})_2] \cdot 2\text{H}_2\text{O}$.

The solid-state structure determined by x-ray diffraction is shown in the figure at upper left. The tetraoxo ion of formula $\text{NpO}_4(\text{OH})_2^{3-}$ displays a highly unusual geometry with four oxo ligands in an equatorial plane and two trans OH ligands, one above and one below this plane. The four planar O ligands have an average Np-O distance of $1.878(5) \text{ \AA}$, and the two Np-OH bonds are $2.238(4) \text{ \AA}$. XAFS spectroscopy was

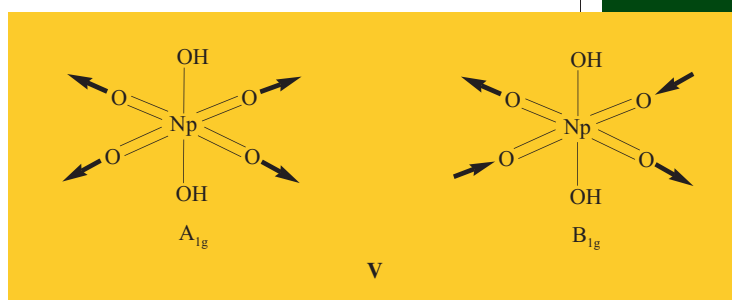
used to determine structural details of the Np(VII) ion both in highly alkaline solution and in the solid state. The figure at lower left shows a representative Fourier transform (without phase corrections) of the k^3 -weighted XAFS spectra, the theoretical fit to the data, and illustrates the single-shell contributions to the fit. These bonding parameters are nearly identical to those found in the crystal structure determination described above.

It is very unusual for a metal ion to have four coplanar oxo ligands as indicated in **III**. For transition metals in their highest oxidation states, the tetraoxo ions of general formula MO_4^- (Mn, Tc, Re) or MO_4^{2-} (Cr, Mo, W) are always tetrahedral as shown in **IV**. In the tetrahedral geometry, all five metal d orbitals can be used to maximize the M–O bonding. The unusual planar arrangement of O atoms in $\text{NpO}_4(\text{OH})_2^{3-}$ can be traced to the presence of $5f$ orbitals and the use of a combination of $5f$, $6d$, and $6p$ orbitals in chemical bonding.

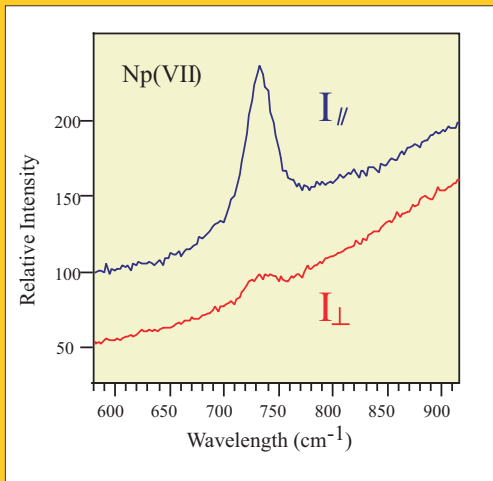
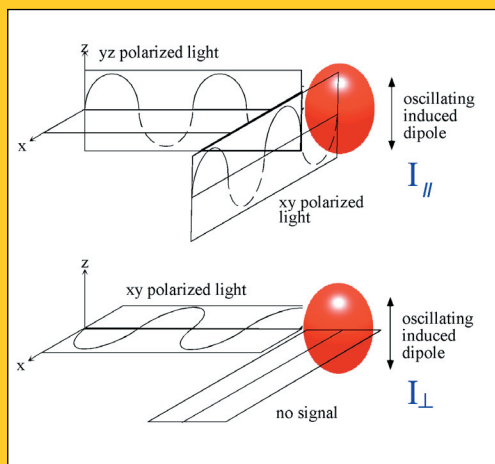


The 1.88 Å Np=O bonds in the planar $\text{NpO}_4(\text{OH})_2^{3-}$ ion are rather long when compared with other Np=O bonds in dioxo species, which average around 1.75 Å for NpO_2^{2+} ions. Transition metal tetraoxo ions are even shorter, as evidenced by the comparison with the ReO_4^- ion, which shows four Re=O bonds at 1.69(2) Å. Thus, the long Np=O bonds observed in $\text{NpO}_4(\text{OH})_2^{3-}$ suggest that the Np=O bond is weakened relative to the Np=O bond in NpO_2^{2+} ions.

To better understand the relative strengths of the Np=O bond in $\text{NpO}_4(\text{OH})_2^{3-}$ we turn to other forms of spectroscopic characterization. Raman spectroscopy can provide sensitive insights into the strength of the M=O bonds and has found wide utility in the study of actinide oxo complexes. The idealized molecular structure of $\text{NpO}_4(\text{OH})_2^{3-}$ possesses D_{4h} symmetry, and this tetraoxo fragment **III** should display two separate vibrations in the Raman spectrum—a totally symmetric mode of A_{1g} symmetry and an asymmetric mode of B_{1g} symmetry, as shown in **V**.



Raman spectra recorded for Np(VII) solutions at varying hydroxide concentrations and in the solid state always showed a single invariant Raman peak. Since it was possible that the two vibrational modes were coincidentally overlapping one another, depolarization ratio studies were used to assess whether the mode we were observing was the totally symmetric (A_{1g}) vibration, the asymmetric (B_{1g}) vibration, or an overlap of the two. Totally symmetric vibrations give rise to polarized Raman lines, whereas nontotally symmetric vibrations give Raman lines that are depolarized.



Polarized Raman spectra of the $\text{NpO}_4(\text{OH})_2^{3-}$ ion identify the vibrational symmetry

A totally symmetric vibrational mode gives rise to a polarized Raman line, and a vibration with lower symmetry is depolarized. When polarized laser radiation is employed, we can monitor the polarization of the scattered Raman line to determine the symmetry of the vibration. This figure shows a solution spectrum of $\text{NpO}_4(\text{OH})_2^{3-}$ recorded with perpendicular and parallel polarization of the exciting laser. The observed frequency is clearly polarized, and can be assigned to the totally symmetric A_{1g} vibration.

In the figure at upper left, a marked decrease is seen in the intensity of the Raman band when observed in a perpendicular as opposed to parallel orientation, thus identifying a symmetric A_{1g} vibration. The decrease in intensity of the A_{1g} band also serves to demonstrate that there was not a B_{1g} band masked underneath this mode, since the B_{1g} band should still be present at full intensity in the figure at lower left. Raman spectroscopy on single crystals also revealed a single A_{1g} vibrational mode identical to that observed in the solution. The reason that we don't observe the asymmetric vibration in our studies is under evaluation, but it is possible that we are observing resonance enhancement of the totally symmetric mode. Additional studies where we vary the frequency of the exciting laser are in progress.

For single-crystal samples, the symmetrical $\text{Np}=\text{O}$ vibrational mode is observed at the extremely low frequency of 716 cm^{-1} , while in 2.2 M LiOH solution this value increases slightly to 735 cm^{-1} . These low vibrational frequencies confirm that the $\text{Np}=\text{O}$ bond is weakened relative to the more common dioxo ions, which show typical $\text{Np}=\text{O}$ stretching modes in the higher-frequency (stronger bonds) range $850\text{--}780\text{ cm}^{-1}$. The longer, weaker bonds observed in the tetraoxo ion are an indication that there is much less π -electron donation from the oxo ligands to the metal center in tetraoxo versus dioxo ions. This assessment is supported by the observation of an ^{17}O NMR chemical shift at $\delta 1470\text{ ppm}$, which can be compared to the value of 1125 parts per million observed for UO_2^{2+} under the same solution conditions.

The theory of NMR chemical shifts is quite complicated, but in general, a lower electron density on an oxygen atom leads to a greater downfield shift. Our data are therefore consistent with the notion that the $\text{NpO}_4(\text{OH})_2^{3-}$ ion has more electron density on the oxygen atom relative to the transdioxo ions. The combination of this data—a long $\text{Np}=\text{O}$ bond, a low ($\text{Np}=\text{O}$) vibrational frequency, and a high-field ^{17}O resonance—all point to weaker bonding in the $\text{Np}=\text{O}$ bonds of tetraoxo ions relative to dioxo ions. Our current efforts are focused on quantifying the relative contributions of σ and π bonding and the relative roles of the $5f$, $6d$, and $6p$ orbitals in forming these bonds in the square planar NpO_4 unit in $\text{NpO}_4(\text{OH})_2^{3-}$.

This research is supported by the DOE Office of Basic Energy Sciences.

The relative roles of 5*f*, 6*d*, and 6*p* atomic orbitals Why UO_2^{2+} is linear and isoelectronic ThO_2 is bent

The UO_2^{2+} ion is well known in actinide chemistry and displays a linear geometry in every known example of its complexes. In contrast, the isoelectronic ThO_2 molecule is bent in the gas phase with an O–Th–O angle of 122° . The theoretical understanding of these differences has taken nearly 20 years to understand fully and hinges on a detailed understanding of the relative roles of the atomic 5*f*, 6*d*, and 6*p* orbitals in forming the metal oxygen bond in these two systems.

In the early 1980s, there were two points of view: one based on U–O π bonding (Bill Wadt at Los Alamos) and another based on U–O σ bonding (Roald Hoffmann at Cornell University). The Los Alamos view was that for U, the 5*f* levels are significantly lower in energy than the 6*d*, while for Th, the 6*d* level is lower than the 5*f*. Theoretical calculations showed that 6*d* π bonding was important for both Th and U, but that U could also use the 5*f* orbitals for π bonding. A bent geometry was preferred for Th due to the dominance of the 6*d* π bonding, and a linear geometry was preferred for U because a linear geometry could use both 6*d* and 5*f* orbitals for bonding. The Cornell point of view,

also based on theoretical calculations, was that U could use a combination of 5*f* and 6*p* (normally considered to be in the core) orbitals to form an unusually strong σ bond in the linear geometry.

Twenty years later and after the application of very sophisticated spectroscopy (two-photon laser and oxygen k-edge x-ray absorption) and more modern theoretical calculations based on the hybrid density functional approach, we have found a resolution of these two points of view. In the final analysis, both σ and π bonding are found to be important. Both *f* π and *d* π bonding occur, but the *d* π bonding is significantly stronger. Moreover, in a strange and unexpected way, we also learned that the *f* σ hybridizes with 6*p* σ , and the resulting *f*-*p* U–O σ bond is much stronger than the U–O σ bond formed by the *d* orbitals. Therefore, the dominant covalent interactions in linear OUO^{2+} are due to the strong 5*f*-6*p* σ bonding and 6*d* π bonding.

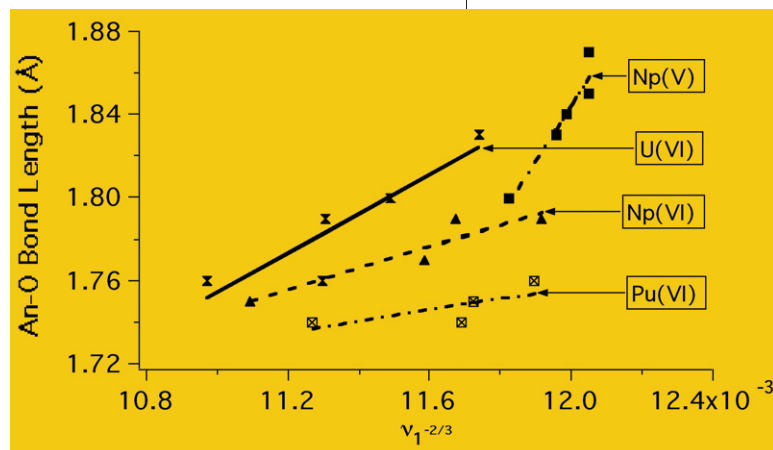
The correlation between Raman spectroscopy and bond lengths in high-valent actinide complexes

This article was contributed by Los Alamos researchers C. Drew Tait, D. Webster Keogh, Mary P. Neu, Sean R. Reilly, Wolfgang Runde, and Brian L. Scott of the Chemistry Division; Robert J. Donohoe of the Biosciences Division; David L. Clark of the Nuclear Materials and Technology Division; Steven D. Conradson of the Materials Science and Technology Division; and Scott A. Ekberg, formerly of the Chemistry Division.

The correlation of vibrational energies to bond strength and molecular structure has a long tradition in inorganic chemistry. For example, Badger's rules allow the metal-metal bond length for second- and third-row transition dimetallic complexes to be predicted based on the bond vibrational energy. In the course of our studies of structure and bonding in actinide complexes in high-oxidation states, we have examined a variety of axial dioxo systems in which the linear $O=An=O$ moiety is both highly sensitive to the electronic configuration of the complex and also yields a characteristic Raman band, identified as the symmetric stretch ν_1 .

With only a handful of crystallographic studies of actinyl complexes available, until recently there has been a relative paucity of the structural data needed for the development of structure/vibrational band correlations. Now, however, x-ray beam-line studies, especially XAFS spectroscopy, are used to characterize the structural properties of solution and polycrystalline actinide samples, creating a much more expansive structural data base for actinide complexes. As a result, we can now correlate the energy of the ν_1 Raman band, either from the literature or our own data, with structural data derived from both crystallographic and solution XAFS studies to seek the common relations between the vibrational energies and An-O bond lengths.

Plots comparing the structural and vibrational data for representative U, Np, and Pu dioxo species are shown in the figure above, where the An-O bond length (y-axis) is maintained between the different actinides to facilitate comparisons. The units on the x-axis reflect the fact that the mathematics of relations like Badger's rule are such that the bond distance is a linear function of the vibrational energy to the $-2/3$ power. Clear trends can be seen within a particular oxidation state of an actinide, for example U(VI) and Np(V); however, unlike dimetallic transition metal complexes, no universal trend between the actinides or even between oxidation states of the same actinide is observed.



The correlation of actinyl bond distance to vibrational energy for a variety of actinide metals and oxidation states.

The sensitivity of Raman band energy to the bond distance (slope) is much greater for Np(V) than for U(VI), which in turn is more sensitive than that observed for Np(VI). Pu(VI) manifests shifts in $\nu_1 > 40 \text{ cm}^{-1}$ even though the changes in the Pu=O bond length are very limited. Thus, for Np(V), bond distance is a more sensitive indicator of changes in the equatorial bonding structure than are the vibrational data, while for Pu(VI) the opposite is true.

Given the successful application of Badger's rule for entire rows of transition metal dimer stretches, the lack of a consistent trend for the symmetric "-yl" stretches, which is also a two-atom motion, is perhaps surprising. Thus, the identity of the actinide itself, its oxidation state, and the equatorial ligand content must all be considered to be of potential influence in determining the combined distance and bond-energy properties of the actinyl structural element.

For example, encompassing dioxo Np(V) into a rather large crown ether minimizes the equatorial (ether) interactions and causes the axial "-yl" bond to be considerably shorter than that for the tris carbonate species, where carbonate interacts very strongly in the equatorial position and engages bonding electrons that might otherwise interact with the axial oxygens. Another means of comparison can be made in terms of *f*-orbital occupancy. Thus, we can find consistency in the structural and vibrational properties of the f^1 configuration complexes of $[\text{UO}_2^+]$ and $[\text{NpO}_2^{2+}]$. However, such comparisons must be carefully made. As an example, the structural and vibrational properties of f^0 dioxo U(VI) complexes cannot be compared with Np(VII) complexes because the latter adopt a tetraoxo core structure.

Comparing the structural and vibrational data from similar complexes of different actinides provides an interesting perspective.

Across the actinide series, for a given oxidation state, the metal atomic radius decreases as the atomic mass increases. This actinide contraction, similar to the well-studied lanthanide contraction, results in the prediction that the metal-oxygen bond length should get shorter as one proceeds along the actinide row of the periodic table.

Such a result is indeed observed in the structural data but yields a surprising correlation with the vibrational energies. Generally, shorter bond lengths yield higher energies for the corresponding stretching mode; however, the opposite relation is found here. A comparison of the Np(V) \rightarrow Pu(V) and Np(VI) \rightarrow Pu(VI) aquo complexes, as well as the U(VI) \rightarrow Np(VI) \rightarrow Pu(VI) tris carbonate complexes and Np(VI) \rightarrow Pu(VI) tetrachloro complexes all show decreasing stretching frequencies accompanying the shorter bonds.

This result can be interpreted as follows. The bonds to the "-yl" oxygens include contributions from the $5f$ orbitals. The primary physical cause of the actinide (and lanthanide) contraction is decreased shielding of the core positive charge across the series: as electrons are added to the outermost frontier orbitals they do a poorer job of screening the charge from the additional protons crowded at the atomic core.

Decreased shielding, in turn, causes the $5f$ orbitals to shrink toward the core, and their directionality decreases as they become more diffuse. Therefore, although the axial oxygens "chase" these orbitals inward across the actinide series (the vibrational potential energy curve minimum moves to a smaller equilibrium distance), their overlap with the increasingly buried $5f$ orbitals still decreases, and the bond order is reduced (the potential energy surface becomes less curved).

Badger's rule

Fundamental manifestations of chemical bonding include the strength of the bonds that are formed as well as their length. Intuitively, there should be a link between the bond strength and the subsequent length of that bond, and this link is provided by Badger-type rules. However, with the vibration viewed as a potential energy curve, the position of the potential energy minimum (bond length) does not necessarily have a unique link to the width/steepness of the potential energy curve (bond strength).

In fact, an example is mentioned in the main article for the tris carbonato species where weaker dioxo bonds are accompanied by shorter bond lengths. Therefore, care must be taken to tune the Badger-type relationships and to test how wide their application is. Many of the Badger-type relationships involve stretches that are described as being due to the vibration of two atoms, as in the case of metal-metal bonding. The linear dioxo moiety involving the early actinides in high-valence states is an uncommon structural motif in chemistry and requires its own Badger-type relationships.

Badger's rule is named for the late Richard McLean Badger, whose career as a student, teacher, and researcher at the California Institute of Technology spanned more than 50 years. His "rule," which relates a change in stretching frequency with a change in bond lengths, was the result of his extensive study the force constant and internuclear distance in a large number of diatomic molecules.

Badger-type relations provide a link between bond strength and bond length, which in turn, provides important constraints to check the theoretical calculations (with their associated approximation methods) performed to inform us of the orbitals used in constructing the molecule. Alternatively, bond lengths of unknown or new molecules can be estimated from vibrational information on the bond strengths. Because growing single crystals for x-ray diffraction studies is difficult and sometimes not possible, this is a valuable tool to have.

This research was supported by a Laboratory Directed Research and Development (LDRD) project administered by the Glenn T. Seaborg Institute of Transactinium Science at Los Alamos National Laboratory. EXAFS experiments were performed at the Stanford Synchrotron Radiation Laboratory, which is supported by the DOE Office of Basic Energy Sciences.

Organometallic actinide chemistry

Developing a comprehensive picture of the chemical behavior of the 5f elements

There has been a recent resurgence of interest in understanding the electronic structure of complexes of the actinide elements. This is driven principally by the desire to predict the behavior of actinide species in a variety of applications within the DOE complex, from waste repositories to the design of selective chemical separation methodologies.

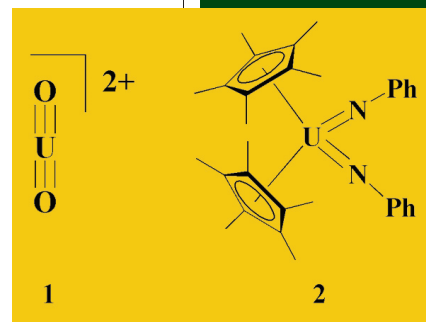
Generally, present models describing the electronic structure of the actinides are most relevant to chemistry performed under aerobic conditions and do not provide a comprehensive set of chemical environments in which to probe characteristics of metal-ligand bonding. To assess the validity of theoretical treatments already developed and ensure that chemical behavior is predictable under a wider array of process conditions, it is important to study a broader range of ligands and chemical environments than those commonly examined and their influence on observable chemical behavior.

Nonaqueous organometallic chemistry provides access to the broadest possible set of ligands with which to examine the influence of coordination environment on the electronic structure and chemical reactivity of the actinide elements. We have chosen to focus particular attention on the generation and investigation of actinide-ligand multiple bonds to probe the potential for involvement of metal 5f electrons in chemical bonding, examine the stability of functional groups isoelectronic with the oxo ligand, and demonstrate reaction patterns unique to f elements.

Nonaqueous analogues to the uranyl ion

The uranyl ion (1) is the dominant form of uranium in aerobic media and features a linear $O=U=O$ fragment with uranium in its highest formal oxidation state, U(VI). More than a decade ago, we prepared the first example of an organometallic U(VI) complex, $(C_5Me_5)_2U(=N-Ph)_2$ (2). This complex was remarkable in that it also represented the first example of a bis(imido) $U(NPh)_2^{2+}$ electronic analogue to the uranyl ion, UO_2^{2+} .

However, unlike the uranyl ion, this uranium complex displays an unusual nonlinear or cis arrangement of the two imido functional groups ($U=N$). The fact that complex 2 contained a bent $N=U=N$ core challenged accepted motifs for bonding in actinide complexes. Complex 2 is a 20-electron species that has no transition metal analogue, raising significant questions about the electronic structure of this compound and in particular the participation of valence metal orbitals (5f, 6d, and 7p) in ligand-to-actinide π bonding.



The uranyl ion (1) and the U(VI) bis(imido) complex, $(C_5Me_5)_2U(=N-Ph)_2$ (2).

This article was contributed by Los Alamos researchers Jaqueline L. Kiplinger of the Chemistry Division and Carol J. Burns of the Office of the Deputy Director for National Security.

ORGANO-
METALLIC
ACTINIDE
CHEMISTRY

We examined the extent of *f*-orbital participation in this hexavalent uranium complex through collaborative interactions with both experimental and theoretical scientists. Bruce Bursten of The Ohio State University and P. Jeffrey Hay of Los Alamos conducted theoretical investigations on simplified model complexes and demonstrated that *5f*-orbital involvement can contribute to the stabilization of nitrogen donors in a manner that is not possible for the transition metals. Jennifer Green of Oxford University confirmed these results, using photoelectron spectroscopy, which revealed a small but significant *f*-orbital-based bonding interaction.

Complex 2 can be prepared by a variety of methods as shown in Scheme 1. The most general route is two-electron oxidative atom transfer using organic azides (RN_3) (e.g., $3 \rightarrow 2$, $5 \rightarrow 2$). Another method that has proven useful in the synthesis of bis(imido) transition metal complexes is the reductive cleavage of 1,2-disubstituted hydrazines, in which the cleavage of hydrazo compounds (R-NHNH-R) allows for the introduction of a single organoimido functional group.

However, the reaction of complex 4 with 1,2-diphenylhydrazine to produce the bis(imido) complex 2 provides the first example of the reductive cleavage of a hydrazo compound yielding two organoimido functional groups at a single metal center. The most unusual chemistry exhibited by these bis(pentamethylcyclopentadienyl) uranium complexes

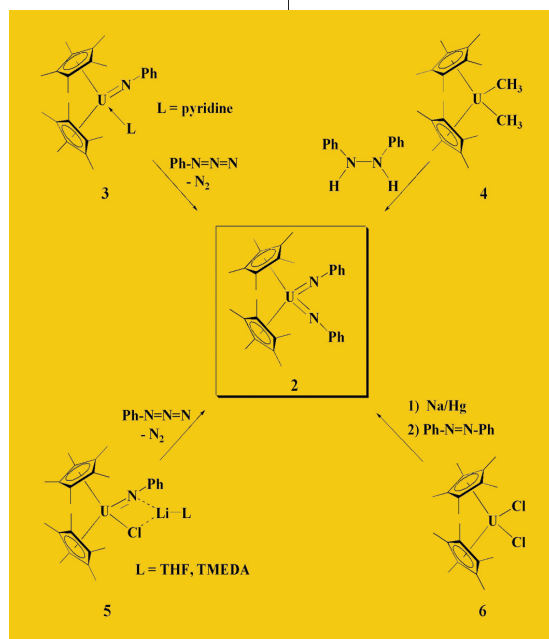
is the four-electron reductive cleavage of the double bond in azobenzene (Ph-N=N-Ph) by $(\text{C}_5\text{Me}_5)_2\text{U}(\text{Cl})(\text{NaCl})$ generated by reduction of complex 6 by Na/Hg to give the bis(imido) complex 2, a process not often observed for transition elements. These reactions, shown in Scheme 1, underscore some differences between the transition metals and the actinides and suggest the possible involvement of the *5f* orbitals in chemical reactions of uranium.

In search of reactive actinide-ligand multiple bonds

One of the most exciting discoveries in organometallic chemistry over the past 15 years was the observation that d^0 transition-metal imido complexes readily react with carbon-hydrogen bonds. Analogous f^0 actinide imido complexes might be expected to display similar reactivity patterns to their early transition-metal counterparts; however, as in the case of uranyl compounds, the most characteristic chemical property of uranium imido bonds is their decided lack of

chemical reactivity.

Recently, we discovered a method to access reactive uranium imido complexes. We found that diazo-alkanes (R_2CN_2) can be used to prepare U(VI) bis(imido) complexes that are reactive toward alkanes, as illustrated in Scheme 2. Reaction of the U(IV) monoimido



Scheme 1. Synthetic scheme for the preparation of the U(VI) bis(imido) complex 2.

complex 7 with diphenyldiazomethane generates the U(VI) bis(imido) complex 8. Complex 8 does not lose N₂ to give a U(VI) alkylidene complex (an alkylidene is a complex possessing a metal-carbon, or M=C, functional group). This is in marked contrast to the chemistry observed for isoelectronic N₂O and organoazides (RN₃), which have been exploited for the preparation of U(VI) oxo (U=O) and imido complexes.

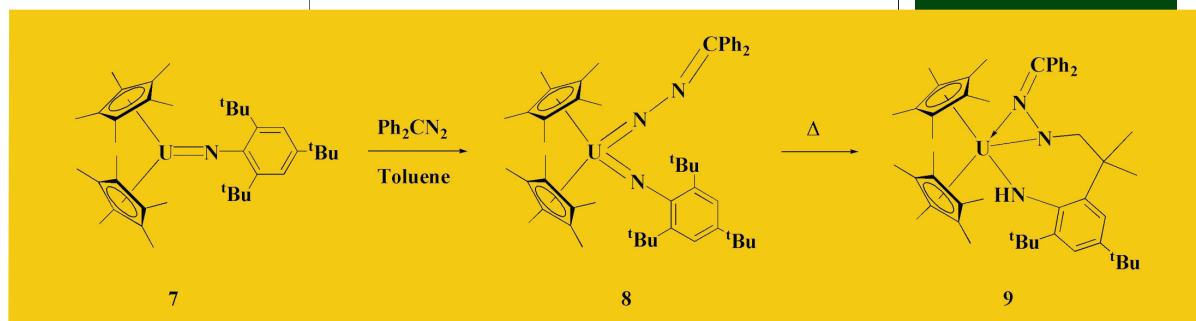
The oxidation of the uranium metal center from U(IV) to (VI) is clearly demonstrated by NMR spectroscopy and electronic absorption spectra of complex 8. The electronic absorption spectrum shows no $f \rightarrow f$ transitions in the near-IR region but does show a broad, intense and featureless charge-transfer band in the visible region, which is consistent with the assignment of an f^0 U(VI) metal center.

The proton NMR spectra of complex 8 is temperature invariant between -75 and 60 °C but displays anomalous chemical shifts, suggesting that complex 8 is a temperature-independent paramagnet, a characteristic property of organometallic complexes of U(VI). An x-ray crystal structure of complex 8 confirmed the presence of two organoimido groups terminally bound to the uranium center and the overall structure of complex 8.

Proton NMR spectroscopy signaled the quantitative formation of the novel cyclometallated U(IV) bis(amide) complex 9 upon thermolysis of a solution of complex 8; the NMR spectrum of the product is paramagnetically shifted, which indicates that the product is a reduced f^2 U(IV) species. X-ray crystallography unambiguously ascertained that the C-H bond of one of the *t*-butyl groups from the

U=N-2,4,6-*t*-Bu₃C₆H₂ fragment in complex 8 has been activated to give complex 9.

This reaction type has no equivalent in transition metal chemistry and represents a new pattern of reactivity available for high-valent actinide imido complexes. The uranium center is bound to three nitrogen atoms. Two exhibit short U-N distances associated with uranium-amide linkages. The remaining U-N

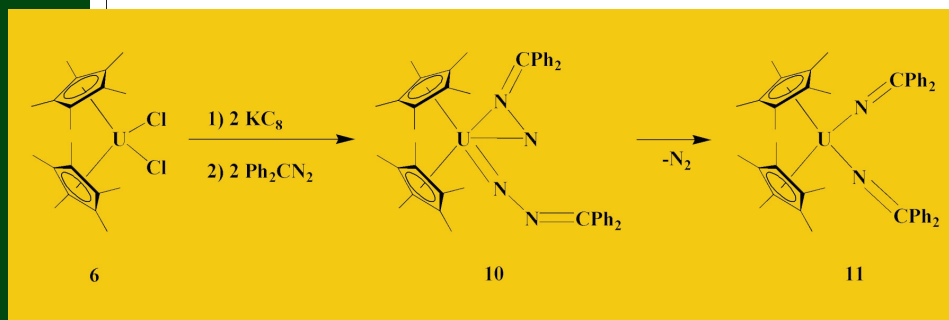


length is consistent with a uranium-nitrogen dative interaction. Notably, the U-N(H)-C fragment is bent, which differs significantly from the nearly linear U-N-C_{ipso} unit present in the parent bis(imido) complex 8.

f-electron delocalization in organometallic actinide complexes

We are also interested in understanding the degree to which valence metal orbitals contribute to bonding and reactivity. Covalency (the mixing of orbitals) in metal-ligand bonding is quite prevalent in transition metal complexes but is suggested to play a reduced role in the chemistry of the actinides. We recently discovered several classes of organo-uranium complexes in which the oxidation state of the metal, and thus the location of the valence electrons, is not easily determined. The spectroscopy, reactivity, and structural chemistry of these compounds suggest that the 5*f* electrons are far more involved in chemical bonding than previously thought.

Scheme 2. Synthetic scheme showing the reaction of the U(IV) monoimido complex 2 with Ph₂CN₂ to generate the bis(imido)U(VI) complex 8, and its thermal transformation into a cyclometallated complex 9.

ORGANO-
METALLIC
ACTINIDE
CHEMISTRY

Scheme 3. Synthetic scheme for the preparation of uranium diazoalkane complex 10 and its transformation into the U(IV) bis(ketimido) complex 11.

We have investigated the reaction chemistry of low-valent organouranium complexes with diazoalkanes, which are known to generate transition metal alkylidene complexes under similar conditions. Reaction of the U(IV) complex **6** with diphenyldiazomethane under reducing conditions generates complex **10** as indicated in Scheme 3. This species is unlike existing transition-metal diazoalkane complexes in that it possesses two diazoalkane molecules bound to a single uranium metal center. One diazoalkane is coordinated to the uranium metal center in an η^1 fashion and forms a uranium imido bond. The second diazoalkane is coordinated to the uranium in an η^2 manner, possibly through the N=N π system.

The exceedingly long N–N bond distance indicates that substantial π backbonding occurs between the $(C_5Me_5)_2U$ fragment and an empty orbital on the diazoalkane unit, which has antibonding character, resulting in a lengthening of the N–N bond. Interestingly, theoretical calculations reveal an $f^1\pi^*$ electronic configuration and suggest delocalization of a $5f$ electron throughout the N=N=C framework of the η^2 -coordinated diazoalkane.

Upon standing in solution, the bis(diazoalkane) complex **10** transforms into the novel uranium bis(ketimido) complex **11**, via loss of N_2 from two diazoalkane fragments. The U–N bond distances are significantly shorter than other structurally characterized U(IV) bis(amido) complexes such as compound **9**.

The nearly linear U–N–C fragments are consistent with the formulation of the ligands as ketimido groups with the metal center accepting additional electron density from the nitrogen lone pairs.

Spectroscopic data suggest donation of electronic density from the metal center onto the ketimido ligands in this system.

Complex **11** is reminiscent of high-valent U(VI) bis(imido) complexes that have significant U–N multiple bond character as typified by complex **2**. The metal center in complex **11** is not U(VI), which is evident upon comparison of the U–N distances in the two systems as well as the NMR and UV-visible-near-IR spectra. The complex is formally an f^2 system, yet it does not behave like known U(IV) amido complexes. The uranium ketimido complex is surprisingly unreactive, displays unusual electronic properties, and is able to support the uranium metal center in a variety of oxidation states ranging from (III) to (V).

The physical properties and chemical stability of this U(IV) complex indicate higher U–N bond order due to significant ligand-to-metal π bonding in the uranium ketimido interactions. The combined data suggest electronic delocalization throughout the N–U–N core and indicate that the $5f$ electrons in midvalent organouranium complexes might be far more involved in chemical bonding and reactivity than previously thought.

The role of f orbitals in reactions of actinides

The role of the $5f$ orbitals in bonding and reactivity is still one of the most intriguing

questions in actinide chemistry and continues to be a topic of considerable debate among theoretical and experimental chemists. The high nodality of the $5f$ orbitals and the expanded electron count of many organoactinide complexes provide the opportunity for the actinide metals to engage in bonding schemes that are not available to the transition metals, leading to new patterns of reactivity. While there is spectroscopic and physical evidence to suggest that f orbitals are key to the stabilization of many high-valent (V, VI) organoactinide complexes, fewer examples of $5f$ orbitals directing reactivity are known in tetravalent actinide chemistry.

In our studies, we have found that diazoalkanes readily insert into both M-C bonds of bis(alkyl) complexes $(C_5Me_5)_2MR_2$ to yield bis(hydrazonato) complexes (see compound **13** as shown in Scheme 4). These 22-electron complexes have no transition metal analogues; the reaction of diphenyldiazomethane with zirconium derivatives affords only mono insertion products. Because transition metals do not have valence f orbitals, these uranium and thorium bis(hydrazonato) complexes provide a unique opportunity to investigate f -orbital participation in the reaction chemistry of organometallic actinide compounds. Theoretical calculations on related model complexes reveal that the $5f$ orbitals interact to a small extent with the N-N π orbitals and the N-N σ orbitals. These results suggest that $5f$ orbitals can contribute to the stabilization of side-bound N-N units for which no appropriate symmetry match exists for transition metals.

Future directions

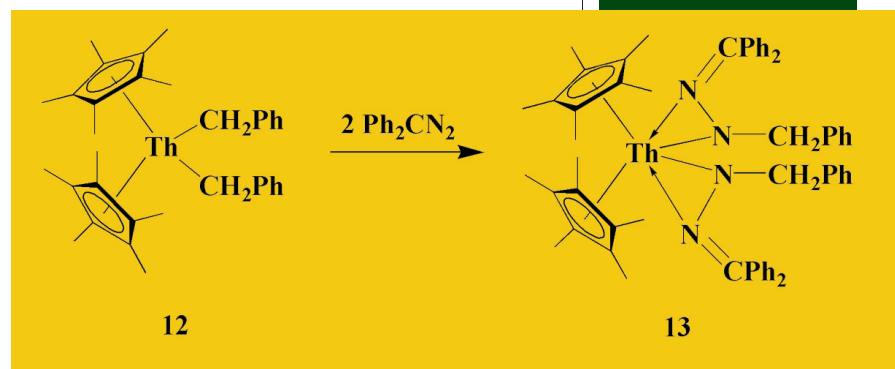
The use of novel ancillary ligand frameworks has provided the opportunity to access complexes in a variety of oxidation states that feature examples of actinide-ligand multiple bonding, yielding a much deeper understanding of $5f$ -orbital energetics and

their involvement in stabilizing metal-ligand multiple bonds. In particular, the observation of "valence-ambiguous" behavior in organo-uranium complexes challenges the once common belief that $5f$ orbitals are energetically inaccessible and serve merely to house unpaired electrons. With our knowledge of the role of both oxidation state and ancillary ligands in stabilizing metal-ligand multiple bonds, it will be possible to extend this work to other as yet unrealized molecular targets, such as species with metal-carbon multiple bonds.

As in the case of actinyl compounds, species containing multiply bound functional groups have most often been found to be unreactive. Recent advances, however, shed light on the means to enhance the reactivity of actinide-ligand multiple bonds, revealing metal-mediated transformations uniquely enabled by $5f$ orbitals. Further studies will explore methods to rationalize and exploit this behavior.

The development of the chemistry of transition metals with multiply bound ligands altered chemists' views of the scope of reactivity possible for these metals. Development of the metal-ligand multiple bond chemistry of the actinides will similarly expand the reach of modern f -element chemistry, while also setting the organometallic chemistry of the actinides apart from that of the transition metals.

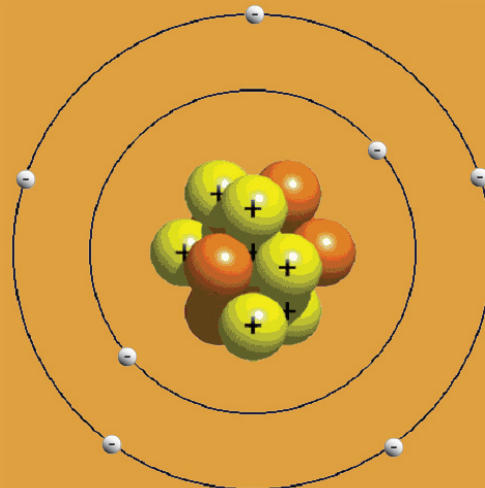
This research is supported by the DOE Office of Basic Energy Sciences.



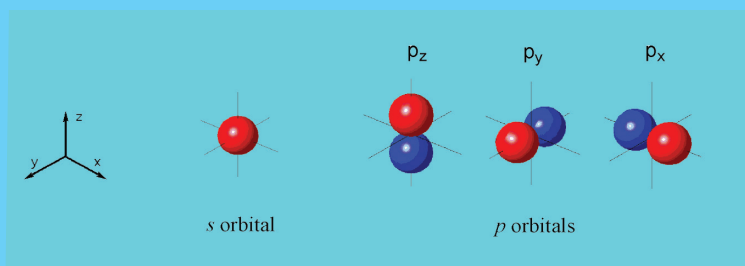
Scheme 4. Synthetic route to the Th(IV) bis(hydrazonato) complex **13**.

What are valence orbitals?

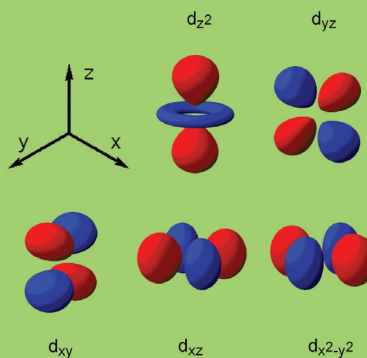
An atom consists of two basic parts: the nucleus and the electrons. The nucleus is the central core of an atom and is made up of protons and neutrons. Electrons are very light, negatively charged particles that surround the positively charged nucleus. Early models of the atom depicted the electrons circling the nucleus in fixed orbits, much like planets revolving around the sun.



Current theory suggests that electrons are housed in orbitals. An orbital is a region of space where there is a high probability of finding an electron. There are four basic types of orbitals: *s*, *p*, *d*, and *f*. An *s* orbital has a spherical shape and can hold two electrons. There are three *p* orbitals, each of which has the same basic dumbbell shape but differ in its orientation in space. The *p* orbitals can hold up to six electrons.



There are five *d* orbitals, which have more complicated shapes than *s* and *p* orbitals. The shape and orientation of the *d* orbitals, which together can hold up to 10 electrons, are shown to the right.



The chemical and physical behavior of the elements results from the configuration of the outermost electrons. These electrons, called the valence electrons, are the most loosely held and interact with those in other atoms to form chemical bonds. The type of orbital (*s*, *p*, *d*, or *f*) that the valence electrons reside in is a function of the elements' position in the periodic table. For example, elements having a partially filled set of *d* orbitals are called transition, or *d*-block, elements. These elements use electrons in the *d* orbitals for bonding and chemical reactivity.

H	s block																p block						He
Li	Be																	B	C	N	O	F	Ne
Na	Mg	d block																Al	Si	P	S	Cl	Ar
K	Ca	Sc	Ti	V	Cr	Mn	Fe	Co	Ni	Cu	Zn	Ga	Ge	As	Se	Br	Kr						
Rb	Sr	Y	Zr	Nb	Mo	Tc	Ru	Rh	Pd	Ag	Cd	In	Sn	Sb	Te	I	Xe						
Cs	Ba	La	Hf	Ta	W	Re	Os	Ir	Pt	Au	Hg	Tl	Pb	Bi	Po	At	Rn						
Fr	Ra	Ac	Rf	Db	Sg	Bh	Hs	Mt	Ds	Uub	Uub												

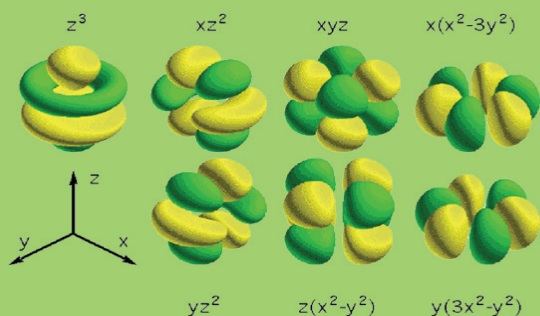
Ce	Pr	Nd	Pm	Sm	Eu	Gd	Tb	Dy	Ho	Er	Tm	Yb	Lu
Th	Pa	U	Np	Pu	Am	Cm	Bk	Cf	Es	Fm	Md	No	Lr

f block

Orbitals are often preceded by numerical designations, i.e. $4f$, $5d$, $3p$, etc. This number is an indication of the size and energy of the orbital. A larger number indicates a larger and higher energy orbital. Thus, electrons in the $3s$ orbital of sodium (Na) are higher in energy and farther away from the nucleus than electrons found in the $2s$ orbital of lithium (Li).

In contrast to the transition elements, the seven *f* orbitals, which are found in lanthanides and actinides, are less well understood. The 14 electrons that can reside in these orbitals are highly contracted (i.e., held close to the nucleus) and are not thought to overlap to any great degree with the valence orbitals of neighboring atoms. Thus, bonding in the lanthanides and actinides is thought to rely more heavily on the *p* and *d* orbitals. As such, the role of the *f* orbitals in bonding and reactivity has been a subject of considerable debate.

-G.G.



Lewis acids and bases

In 1923, J.N. Bronsted and T.M. Lowry independently suggested that acids be defined as proton donors and bases as proton acceptors. Thus, an acid-base reaction is simply the transfer of a proton (H^+) from an acid to a base. The usefulness of this definition lies in its ability to handle any solvent containing protons such as ammonia (NH_3) or sulfuric acid (H_2SO_4).



solvent acid base

Water is a unique species that can act as either an acid or a base.



acid base



base acid

A more general definition of acids and bases was set forth by G.N. Lewis, who defined an acid as an electron-pair acceptor and a base as an electron-pair donor. While encompassing the examples shown above, the Lewis definition includes reactions in which no hydrogens are involved. Neutralization in the Lewis theory consists of the formation of a new bond and includes the generation of acid-base adducts such as $R_3N:BF_3$.



acid base

The solvation of metal ions and the formation of coordination compounds are also examples of acid-base reactions in which the metal ion acts as an acid and the solvent (or ligand) acts as a base.



acid base



acid base

Lewis' definition of acids and bases is widely used because of its simplicity and wide applicability.

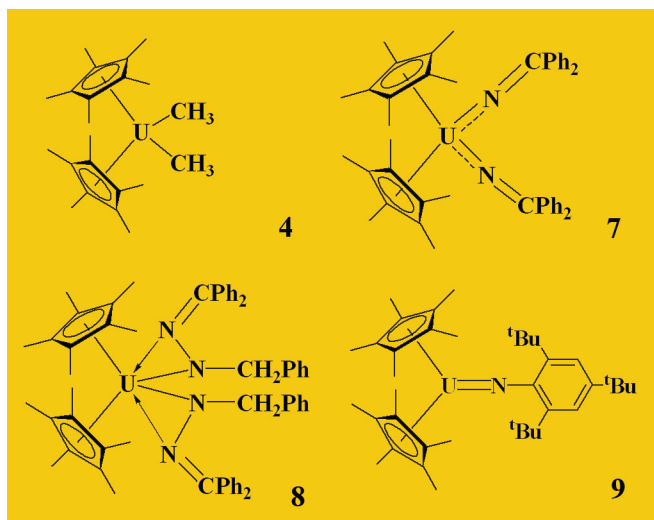
—G.G.

New perspectives from organometallic chemistry
**Electronic structure and bonding
 in 5f-element complexes**

The electronic structure in discrete molecular systems containing actinide metals is dominated by states made up from the seven 5f orbitals on the actinide ion. These 5f orbitals possess a host of interesting properties. From a chemical and electronic structure perspective, one of the more interesting aspects of the 5f orbitals is their radial extension from the nucleus. This is a very important consideration in the formation of chemical bonds. Only those orbitals that extend to the periphery of the atom are actively engaged in direct chemical bonding.

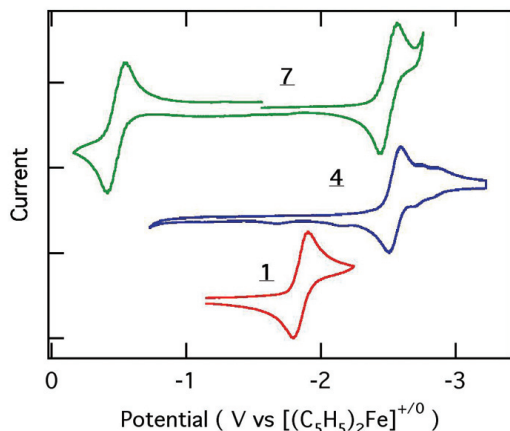
Because of this increased spatial extension of the 5f orbitals, electrons in these orbitals are much more strongly influenced by the presence of neighboring atoms in the actinide-containing molecules than, for example, the 4f electrons in the molecules of the lanthanide series metals. Thus, the measurable properties of the electrons in these 5f orbitals will provide direct information on the other atoms, ions, and/or molecules in the immediate coordination environment of the actinide metal. In fact, the spatial extension of the 5f orbitals provides an opportunity for them to overlap directly with the orbitals on these neighboring atoms. This type of orbital overlap, referred to as a covalent bonding interaction, has been the subject of debate in actinide chemistry for decades.

Much of our understanding of the relationship between electronic structure and chemical bonding in actinide molecules comes from investigations of classical coordination compounds such as the halide salts (e.g., UCl_4). These studies have been invaluable and have laid the foundation for interpretation of spectral data. However, to further our understanding of the more subtle



To help us achieve our objectives in understanding electronic structure and bonding in the actinides, we are creating and investigating an entirely new class of actinide molecules derived from organometallic chemistry. Here we show four different types of structures that we have developed and are investigating. All of these are based on the $(\text{C}_5\text{Me}_5)_2\text{U}$ core (represented by the two pentagons connected to the U metal center). The simplest molecules are typified by (4), which contains two methyl (CH_3) groups bound to the metal. The more interesting systems contain ligands that can bind to the metal in unusual ways—like the ketimide ligands (7) that possess a metal-nitrogen bond of ~ 1.5 , the hydrazone ligands (8) that each have two nitrogen atoms bound to the metal, and the imido ligands (9) that have a bona fide double bond between the metal and the nitrogen atom on the ligand.

This article was contributed by Los Alamos researchers David E. Morris and Jacqueline L. Kiplinger of the Chemistry Division.

STRUCTURE
AND BONDING

Cyclic voltammetry provides information about the energy required to add or remove electrons from molecules by scanning the potential in a cyclic fashion and measuring the current that results. Peaks in the current response (positive for addition of electrons, negative for removal of electrons) signal the onset of electron transfer, and the potential at which these peaks occur provides a relative measure of the energy of the process. Here we show voltammetry for three molecules. Complex 1 (red) only exhibits a single wave (the terminology for a combined positive and negative peak that are slightly offset from each other in potential) at ~ -1.8 V assigned to the U(IV) / U(III) transformation in this complex. Complex 4 (blue) has similar features but at more negative potential values. (Note that voltammograms are plotted with more negative potentials to the right.) Complex 7 (green) exhibits a wave at ~ -2.5 V for U(IV) / U(III) and a wave at ~ -0.5 V. This additional wave is assigned to a U(IV) / U(V) oxidation process. This new wave signals the onset of new bonding features associated with the nitrogen-containing ligands.

aspects of the electronic/molecular structure link and to explore in greater detail the existence of direct 5f-orbital participation in bonding, we need to access chemical systems that allow greater control over and variability in the molecular structure.

Organometallic actinide chemistry provides an opportunity to exercise precise control over the structure of the coordination environment around the actinide ion, while also allowing the introduction of a broader range of ligands than possible in classical coordination chemistry. Thus, in addition to classical ligands like the Cl⁻ ion, unusual ligands can be introduced that are capable of participating in both σ and π bonding with the metal center. We recently investigated the electronic structure and bonding in a series of tetravalent organouranium complexes of the general formula $(C_5Me_5)_2U(R)(R')$ where R and R' are ancillary ligands including halide, triflate, alkyl, imido, hydrazonato, and ketimido.

Two of the most useful experimental probes of electronic structure in discrete molecular systems are electronic absorption spectroscopy and electrochemistry, in particular cyclic voltammetry. The former technique, also commonly referred to as UV-visible-near-infrared or optical spectroscopy, provides information about the energies and intensities of transitions between the electronic states in a molecule. For the organoactinide complexes, we will be interested in transitions between the electronic states derived from the 5f orbitals and between states derived from electron excitations from these 5f orbitals to other molecular orbitals, both metal- and ligand-based.

Voltammetry is based on the addition or removal of electrons from molecules at a solution/solid electrode interface. Because these electron transfer processes occur *from* the highest occupied orbitals (oxidation) or *to* the lowest unoccupied molecular orbitals (reduction), this technique gives a direct measure of the stability of the oxidation state of the parent complex and the energy to change that oxidation state by \pm one or more electrons. Ideally, the trends in the data provided by both experimental probes can be related back to trends in structural variations to obtain a deeper understanding of the influence of molecular structure on electronic structure.

Redox properties from cyclic voltammetric studies

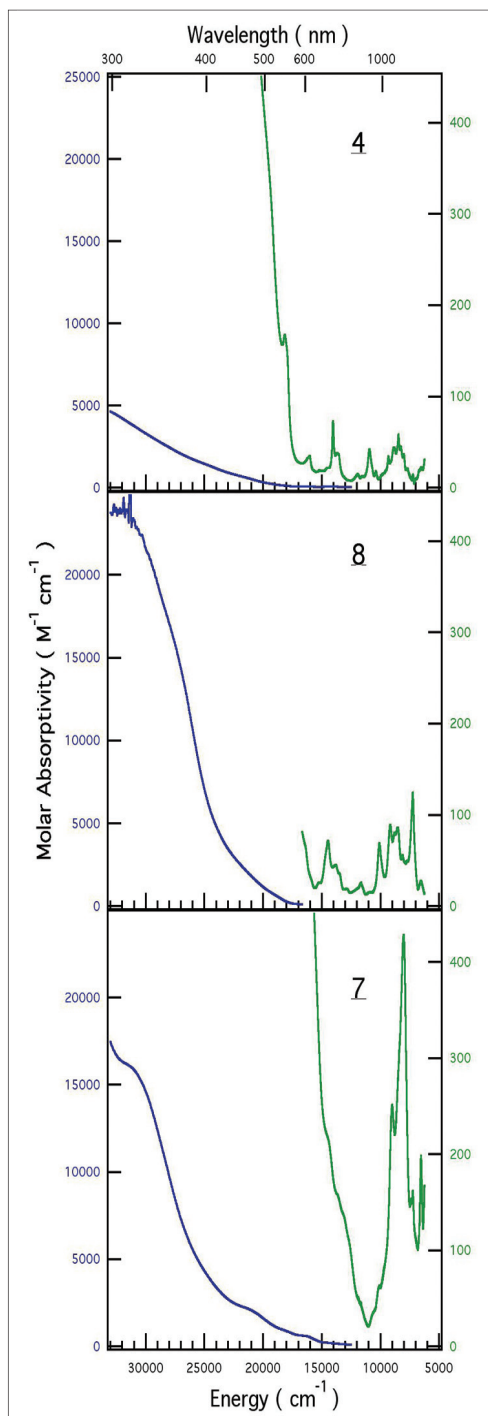
To investigate the influence of the ancillary ligands (R, R') on the energetics of the metal-based redox couples, we focused on the redox waves attributable to the uranium metal-based processes. All of the complexes can be classified into only two categories: Category 1 includes complexes where R and R' are chloride, alkyl, or triflate groups; Category 2 includes complexes where at least one of the R or R'

groups is a hydrazone, imido, or ketimido nitrogen donor ligand.

The ancillary ligands in the Category 1 complexes are all principally σ donors, and the voltammetry in this category is dominated by a single reduction process from U(IV) to U(III) that occurs between ~ -1.8 and -2.7 V versus $[(C_5H_5)_2Fe]^{+/0}$. A useful comparison is the variability in the U(IV)/U(III) redox potential for differing ligand sets. For example, it has been shown that the uranium metal center becomes more difficult to reduce in the series $(C_5H_5)_3UCl < (C_5H_5)_4U < (C_5Me_5)_2UCl_2$. This corresponds to the stabilization of the tetravalent oxidation state due to the electron-donating ability of the ligands, with donor strength decreasing from $C_5Me_5^-$ to $C_5H_5^-$ to Cl. For the Category 1 members, the reduction potential reflects the more strongly electron-donating nature of the alkyl groups relative to the chloride ion. No complexes in the first category show any evidence for a metal-based oxidation process (i.e., U(IV) to U(V)).

All complexes in Category 2 contain one or two nitrogen-containing ligands that have the ability to interact with the metal center in both σ and π modes via the nitrogen lone pair orbitals and/or the π orbital system on the ligand (for the hydrazone complexes). All these Category 2 complexes exhibit a reversible reduction wave at potentials between ~ -2 and -2.6 V that is attributable to a metal-based U(IV)/U(III) process. The distinguishing feature of these Category 2 complexes is the appearance of an oxidative process in the region from $\sim +0.1$ to -0.6 V. The U(V) species appears to be stable on a voltammetric time-scale, with no evidence for chemical reactivity such as disproportionation.

The nitrogen ligands in the Category 2 complexes provide the same measure of stabilization of tetravalent uranium as do the alkyl ligands in the bis and tris alkyl complexes in Category 1. Thus, the potential



Electronic absorption spectra provide us with important information about the energies required to promote electrons between various states within the molecules. For the actinide molecules studied here, there are two important yet distinct types of transitions that occur in different energy regions. The first, shown in green, are associated with changes in electronic states derived from the actinide 5f orbitals. The second, shown in blue, derive from transition in which the electron is promoted from an orbital localized on one portion of the molecule (for example, the metal) to another. We are currently attempting to develop theoretical justifications for the observed differences in molar absorptivity for these transitions in the structurally different complexes (4, 8, and 7). We believe these intensity differences are a direct indicator of the extent of covalent interaction between the uranium metal center and the ligands.

STRUCTURE
AND BONDING

of the U(IV)/U(III) couple is shifted to quite negative values compared, for example, to the bis halide. However, in the case of the nitrogen ligand complexes, the metal center becomes so electron rich that the one-electron oxidation process is also readily accessible and yields a stable pentavalent complex. The difference between these Category 2 complexes and those in Category 1 is the ability of the nitrogen ligands to engage in π bonding with the metal center. Undoubtedly, in the complexes with imido, ketimido, or hydrazonato ligands, the stability of the pentavalent oxidation state derives from the additional π interaction between these nitrogen ligands and the metal center, stabilizing the high valent oxidation state in a way that simple σ -donor ligands alone cannot.

One of the more interesting trends in the redox energetics is that in the Category 2 complexes the potential separation between the U(V)/U(IV) couple and the U(IV)/U(III) couple remains nearly constant over the entire series of complexes (~ 2.1 V). A similar potential separation has been found in most of the other published voltammetric studies of U(IV) metallocene complexes having both U(V)/U(IV) and U(IV)/U(III) couples. Thus, it appears that this potential separation is consistent across most U(IV) cyclopentadienyl complexes having high electron density at the metal center and is not a strong function of the nature of the ancillary ligands.

Electronic structure and properties from optical spectroscopies

The UV-visible-near-infrared electronic absorption spectra for these $(C_5Me_5)_2U(R)(R')$ complexes all have two different energy regions of interest. The first region, which lies in the energy region below $\sim 15,000$ cm^{-1} , contains the electronic transitions between the states derived from the $5f^2$ electronic configuration

($f-f$ bands). The second region lies at energies above $\sim 15,000$ cm^{-1} . In general, this region will contain transitions derived from promotion of a $5f$ electron into higher energy metal-based $6d$ orbitals as well as transitions to ligand-based nonbonding and antibonding orbitals. These latter transitions are referred to as metal-to-ligand charge transfer (MLCT) because the electron is transferred from a metal-based orbital onto an orbital localized on a ligand.

These electronic spectral data also fall into distinct classes related to the nature of the ancillary ligands on the $(C_5Me_5)_2U$ core. The first class of complexes includes those that have ancillary ligands of essentially σ -donor character. All of the complexes in this class have a large number of narrow bands in the $f-f$ region at similar energies. The most important distinguishing characteristics of the spectra for this class of complex are the relative weakness of both the $f-f$ bands and the less-well-resolved, higher-energy bands associated with $f-d$ and MLCT transitions.

The second class of complexes contains a hydrazonato ligand. For complexes in this class, there is also a high degree of similarity in the number and energy of the bands in the $f-f$ region of the spectra, as well as in the broad, poorly resolved bands in the high-energy region. For spectra in this class, however, the intensity of the bands in the $f-f$ region is on average about 50% greater than for those in the class discussed above, and for the broad band in the higher energy region, the intensity has increased dramatically.

The final class of complexes includes the imido and ketimido complexes. For spectra in this last class there is an apparent decrease in the number of $f-f$ bands in the low-energy region. The higher-energy region becomes significantly more structured, although the bands remain unresolved. The $f-f$ bands are even more intense in this class, and the bands in the higher-energy region are comparable in

intensity to those in the second class. Notably, the higher-energy bands extend to much lower energy in the spectra for this class than in those of the previous two classes.

The intensity variation across these three classes of spectral data sets is clearly the most interesting and significant result. The intensities of the $f-f$ bands for the first class of complexes are nominal for actinide complexes having a $5f^2$ electron configuration, and reflect the Laporte spin-forbidden character of these transitions. The substantial increase in intensity observed in the $f-f$ bands for the second and third classes suggest the presence of a new intensity-generating mechanism. The existence, intensity, and energetic proximity of the broad, unstructured, higher-energy bands in these spectra appear to hold the key to this unusual trend in intensity behavior in the $f-f$ bands.

We propose that the increase in intensity in the $f-f$ bands for the second and third class of complexes is a direct result of an intensity-stealing mechanism in the $f-f$ transition moment integral due to coupling of these electronic states to the higher-energy MLCT states in these nitrogen-containing complexes. This type of intensity-stealing mechanism reflects a significant degree of covalency in the bonding between the metal and ligand responsible for the charge-transfer transition. The extent to which the mechanism adds intensity to the $f-f$ transitions is also related to the energetic separation between the metal-based states and the charge-transfer states. The closer in energy the states, the stronger the coupling and the intensity-stealing process.

The key feature of the present series of uranium metallocene complexes that has made it possible to readily identify this interesting electronic phenomenon is the incorporation of nitrogen-bearing ligands. These ligands introduce low-energy, ligand-based orbitals that engender the lower energy charge-transfer

transitions to facilitate coupling. The ligands also provide a mechanism for enhanced covalent interaction with the metal center because of the presence of π orbitals of proper symmetry to mix with the metal f orbitals. Thus, they provide a direct experimental observable (the $f-f$ band intensities) for the degree of covalent interaction between the metal f orbitals and the ancillary ligands. The increase in intensity in the $f-f$ bands in the third class of complexes reflects the fact that the MLCT transitions for these complexes extend to much lower energy and can therefore interact more strongly with the $f-f$ states.

Conclusions

Important trends have been identified in both the electrochemical and the spectral data for these organouranium complexes. Furthermore, these trends are very much related to each other. The voltammetric data illustrate that the nitrogen-bearing ligands result in greater electron density at the metal center, destabilizing the U(III) oxidation state and significantly stabilizing the U(V) oxidation state. These same ligand systems also induce increased intensity in the metal-based $f-f$ transitions by providing an intensity-stealing mechanism that reflects stronger coupling to the charge-transfer excited states and indirectly demonstrates a greater degree of covalency in the metal-ligand bonding than is observed in the σ -donor ligand systems. Ultimately, these studies demonstrate that these important trends can be most readily identified when synthetic methodologies are available to provide a broad range of coordination environments to investigate.

This research is supported by the DOE Office of Basic Energy Sciences.

Provides a powerful examination of complicated mixtures of elements

XAFS spectroscopy as a probe of actinide speciation with oxygen ligation

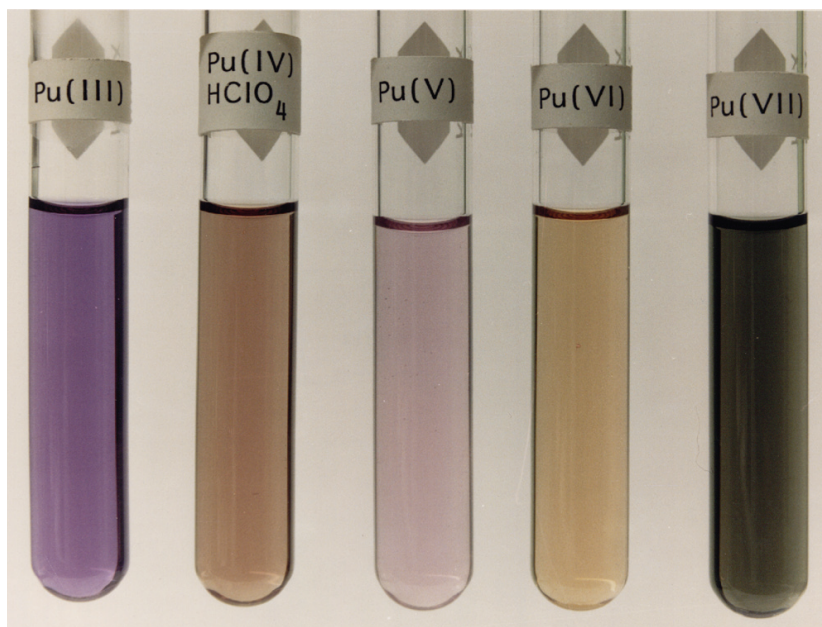
One of the more fascinating characteristics of the coordination chemistry of the light actinide elements is the wide range of oxidation states (or valence) that they exhibit, coupled to a correspondingly broad span of structure, bonding, and reactivity. In its typical location at the extreme of behavior, plutonium in aqueous solution can be found in oxidation states from III to as high as VII, and under the appropriate conditions at low pH, oxidation states III, IV, V, and VI can coexist.

One of the most incisive methods that has been used for probing the structures associated with this chemistry is x-ray absorption fine structure (XAFS) spectroscopy. X-ray absorption techniques have a variety of advantages for the study of plutonium in diverse matrices. Every element absorbs x-rays at a different, characteristic energy that increases with atomic number (Z), giving XAFS a high degree of element selectivity. In some samples x-ray fluorescence from other elements can interfere with the signal of interest. In that case, one can move from examination of the L_{III} edge to another edge (or characteristic absorption energy) in the L shell, such as L_{II}, or L_I. This flexibility makes XAFS very powerful for examination of complicated mixtures of elements.

With third-generation sources, XAFS can be measured to the parts per million concentrations of plutonium typical of many residues. For standards, only a few milligrams of plutonium yield optimum spectra. Such small sample sizes are beneficial when dealing with radioactive materials both to limit radiation exposure to the research scientist and to limit the hazard to the environment and the public.

Furthermore, the x-rays can be focused, allowing spot sizes of several microns in diameter instead of the typical 1.5 by 12 mm size of the native beam. This focusing, in addition to allowing microquantities of plutonium to be probed, can be used to do spectromicroscopy that allows pinpointing or rastering selected areas and imaging versus averaging of the chemical environment across a sample.

The photograph shows the aquo ions of Pu in 1M perchloric acid solution. Pu(V) is in sodium perchlorate solution at pH=7 and Pu(VII) is in 2.5M sodium hydroxide solution.



This article was contributed by Los Alamos researchers Steven D. Conradson of the Materials Science and Technology Division and David L. Clark of the Nuclear Materials Technology Division.

Plutonium has a high affinity for oxygen-containing molecules and it is therefore important to understanding the fundamental coordination chemistry and properties of plutonium-oxygen bonds. From this perspective, the plutonium aquo ions are the “baseline” plutonium species in aqueous solution because they only have water molecules as ligands to the central plutonium ion. Other species form as different ligands substitute for one or more of the water molecules in the coordination sphere of the plutonium ion.

Knowing the characteristics of the aquo ions in detail can provide a starting point for understanding other plutonium complexes. The aquo ions of plutonium in the (III) and (IV) oxidation states have the general formula $\text{Pu}(\text{H}_2\text{O})_n^{3+}$ and $\text{Pu}(\text{H}_2\text{O})_n^{4+}$, respectively, which are often designated simply as $\text{Pu}^{3+}(\text{aq})$ and $\text{Pu}^{4+}(\text{aq})$. But plutonium in the (V) or (VI) oxidation state has such a large positive charge that, in aqueous solution, it extracts the O from water to form the transdioxo (plutonyl) cations PuO_2^+ and PuO_2^{2+} . The corresponding aquo ions therefore have the general formulas $\text{PuO}_2(\text{H}_2\text{O})_n^+$ and $\text{PuO}_2(\text{H}_2\text{O})_n^{2+}$, which are conveniently designated as $\text{PuO}_2^+(\text{aq})$ and $\text{PuO}_2^{2+}(\text{aq})$.

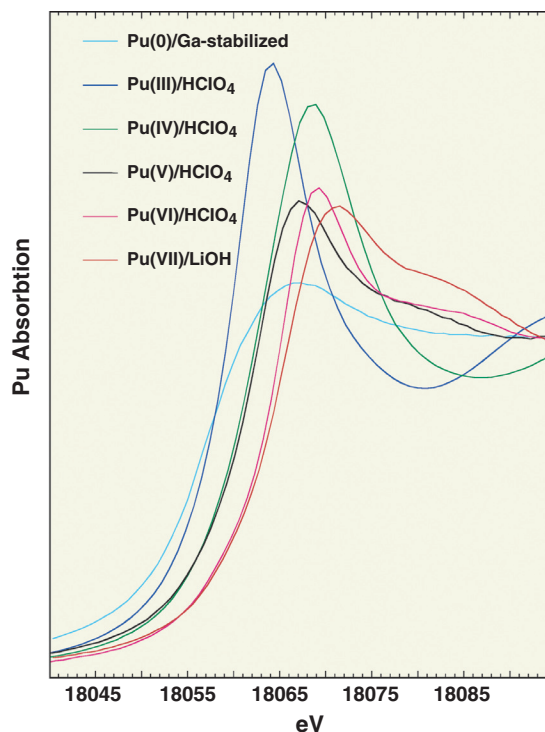
Because the chemical environment surrounding the plutonium ion in each solution is very consistent (the only ligands are water molecules), we could look for behavioral or structural trends among the four oxidation states. Plutonium in the (VII) oxidation state is a powerful oxidant and can only be stabilized for study in alkaline solutions, where its reaction with water is thought to produce a tetraoxo anion of formula $\text{PuO}_4(\text{OH})_2^{3-}$.

Identifying oxidation states

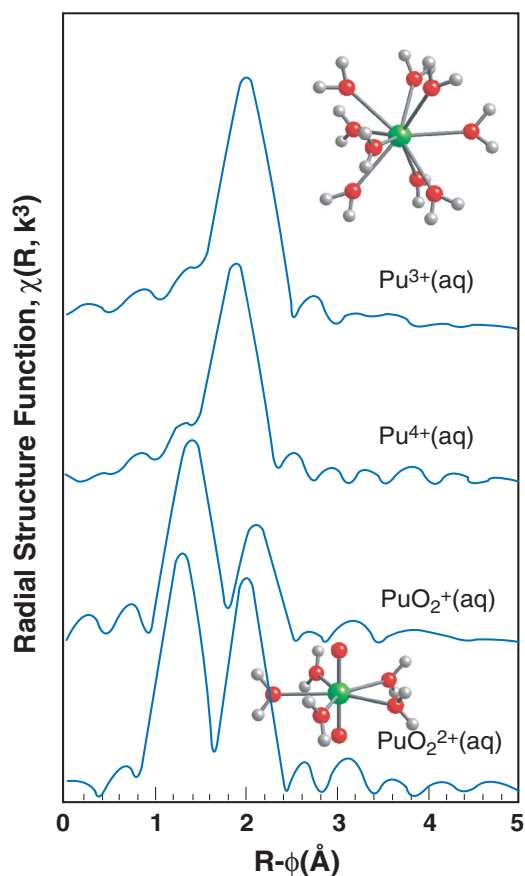
There is structure to the x-ray absorption spectra and this x-ray absorption near-edge structure (XANES), consisting of the absorption edge, the absorption peak, and fine structure on (or before for some transition metals)

these two primary features, can be used to determine the oxidation state of the target (x-ray absorbing) element in solution or the solid state. The exact energy at which these features appear depends on the ionization energy of the ion.

This ionization energy increases with the ion's actual charge, so in general the XANES shifts toward higher energy with increasing valence. We have observed this shift in the plutonium aquo ions. The figure below shows a detailed view of the XANES spectra for a plutonium alloy, Pu(0); the aquo ions of Pu(III), (IV), (V), and (VI) all in perchloric acid solution; and Pu(VII) in a lithium hydroxide solution. The shift in energy between successive oxidation states is clearly visible, with the exception of the spectra of the Pu(IV)–(V) complexes where there is actually a small negative shift.



In this XANES spectra of Pu(0) and the aqueous species of Pu(III)–Pu(VII), the absorption edge shifts toward higher energy and increases as a function of oxidation state. The change in energy between $\text{Pu}^{4+}(\text{aq})$ and $\text{PuO}_2^+(\text{aq})$ is quite small or even negative, reflecting a decrease in the actual charge on the plutonium in the plutonyl(V) species, but the two oxidation states can easily be distinguished by other features, such as the “-yl” shoulder in the XANES spectrum.

ACTINIDE
SPECIATION

In the image above, the Fourier transforms of the EXAFS of $\text{Pu}^{3+}(\text{aq})$ and $\text{Pu}^{4+}(\text{aq})$ —the top two blue lines—show only one major peak, which indicates that all the oxygen atoms of the water ligands lie in a single coordination shell. The amplitude of the peak indicates between eight and nine oxygen atoms per shell. The bond length between (III) and (IV) complexes contracts by 4% with the increase in charge, whereas the number of ligands stays roughly the same. The molecule in the upper right shows a possible structure for $n = 9$, the tricapped trigonal prism. The Fourier transforms of the EXAFS of $\text{PuO}_2^+(\text{aq})$ and $\text{PuO}_2^{2+}(\text{aq})$ —the bottom two blue lines—show two large peaks, which indicate two well-defined coordination shells. The first peak corresponds to the two oxygen atoms of the plutonyl moiety, which are located at 1.74 Å from the central plutonium ion. The second peak corresponds to the oxygen atoms of the water ligands, which are located about 2.4 Å from the central plutonium ion. The equatorial coordination of the Pu(V) complex compared with the Pu(VI) complex shows a significantly smaller number of water ligands, which are located at a longer distance. The molecule in the lower right shows a possible structure for $n = 5$ water ligands, the pentagonal bipyramid.

Other parts of the XANES, however, can be used to help correlate a spectrum with an oxidation state. For example, the shoulder that appears just after the main absorption peak in the spectra of Pu(V) or (VI) complexes in solution—the “actinyl” (or “-yl”) shoulder—can be used to distinguish those oxidation states from Pu(IV). We have observed nearly identical plots for other plutonium species with oxygen ligand environments—including plutonium nitrates, carbonates, carboxylates, and oxides—in solution and the solid state. (In fact, other than the ~450 eV shift in the ionization energy as Z changes, we observe nearly identical spectra for uranium and neptunium compounds as well.)

Because the edge energies are independent of the chemical form of the plutonium, they can be used to identify the oxidation state of plutonium complexes in unknown chemical matrices. There is still speculation about the underlying reason behind the small shift between the (IV) and (V) oxidation states. The shift toward higher energies depends on the actual charge of the ion, rather than its “formal” valence, and evidently the actual charge does not vary much between the two states.

One possible explanation is linked to the formation of the plutonyl cations. The plutonyl cations have a linear structure, $\text{O}=\text{Pu}=\text{O}$. Recent calculations have shown that bonding between the plutonium and oxygen atoms in the plutonyl has a substantial covalent character, reducing the actual charge of the central plutonium ion. The actual charge of the plutonium ion in the Pu(V) complex $\text{PuO}_2^+(\text{aq})$ may therefore be very similar to the actual charge of the plutonium ion in $\text{Pu}^{4+}(\text{aq})$.

The structure of plutonium aquo ions

While changes in the local chemical environment surrounding plutonium have little effect on the XANES, they do have a significant effect on the oscillations in the absorbance that occur at energies beyond the edge. In fact, the local molecular structure can be determined from these oscillations, known as extended x-ray absorption fine structure (EXAFS). Data from the EXAFS region provide information about the local atomic-scale environment.

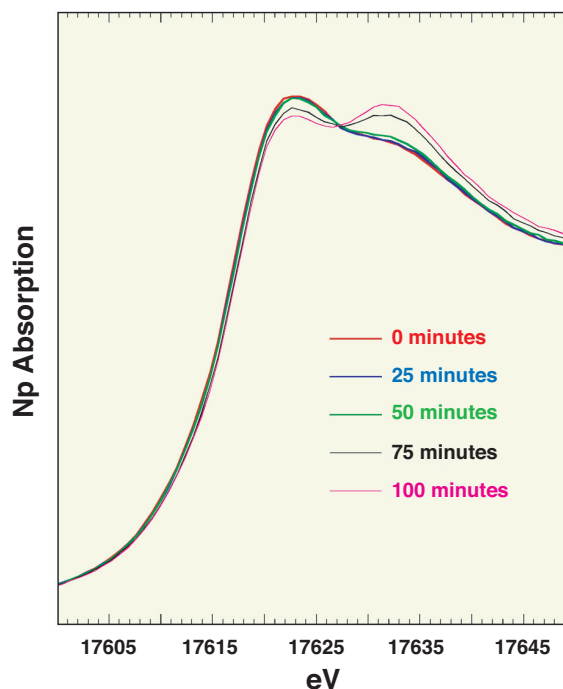
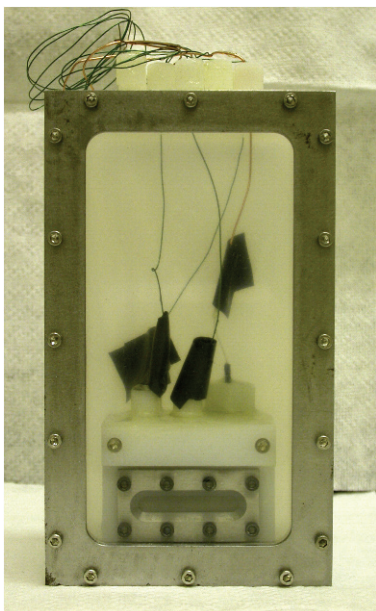
For simple structures with well-separated shells of neighbor atoms, a Fourier transform of the data results in a (phase-shifted and inverse distance-squared weighted) radial distribution function that can be interpreted as shells of near-neighbor atoms surrounding the central metal ion. The position and intensity of the peaks in the Fourier transform are related to the absorber-scatterer distance and the number of atoms in each shell.

The figure on page 38 shows the Fourier transforms of EXAFS data for plutonium aquo ions in oxidation states (III)–(VI). For $\text{Pu}^{3+}(\text{aq})$ and $\text{Pu}^{4+}(\text{aq})$, the data show only a single large peak, which indicates that all the nearest-neighbor atoms (the oxygen atoms of the water ligands) lie evenly dispersed at the same distance from the plutonium ion. All of these results were confirmed by curve-fitting analysis, which also showed a Pu–O distance of approximately 2.49 Å for the (III) state and 2.39 Å for the (IV) state. The shorter bond lengths for the (IV) state are associated with the higher charge of the central ion. The number of water molecules bound to the plutonium is similar for both species, with $n = 8$ or 9. (The $\text{Pu}^{3+}(\text{aq})$ ion with $n = 9$ has been isolated and characterized in the solid state, see the article on page 7.)

The transform of $\text{PuO}_2^+(\text{aq})$ and $\text{PuO}_2^{2+}(\text{aq})$ data shows two peaks. The first corresponds

to the two oxygen atoms in the plutonyl ion. Analysis of the data indicates a Pu=O distance of 1.74 Å. The second peak in the Fourier transform corresponds to the oxygen atoms of the water ligands. It is known from other studies that all these oxygen atoms bond in the equatorial plane of the plutonyl moiety, and we deduce Pu–O distances that range from 2.4 to 2.5 Å.

A significant result of our research is the finding that the $\text{PuO}_2^+(\text{aq})$ has a lower number of water ligands ($n = 4$ to 5), all at a longer bond distance, than $\text{PuO}_2^{2+}(\text{aq})$, where $n = 5$ to 6. This finding confirms a trend that was seen in studies of the actinyl ions of uranium and neptunium, namely, that An(V) species appeared to coordinate fewer ligands than An(VI) species. Because plutonium exhibits aquo ions in four oxidation states, our experiments are the first to observe this trend directly.



To overcome the problem of samples having to be prepared at Los Alamos but studied at a synchrotron located a thousand miles away, researchers developed an electrochemical cell (left) where they could prepare samples in situ at the beam line. The series of XANES measurements (right) show the successful conversion of Np(VI)–(VII).

ACTINIDE
SPECIATION

When other information is taken into account, the XAFS data are consistent with a bipyramidal coordination geometry for $\text{PuO}_2^+(\text{aq})$ and $\text{PuO}_2^{2+}(\text{aq})$. The plutonyl moiety forms the axis of the bipyramid, and, depending on conditions and the ligand used, the geometry may be a tetragonal bipyramid (four ligands in the equatorial plane), a pentagonal bipyramid (five ligands), or a hexagonal bipyramid (six ligands with bidentate species such as CO_3^{2-}). We have used the plutonium aquo ions to establish the baseline data and oxidation state trends necessary to determine the oxidation states of plutonium complexes in matrices of unknown composition. This background data and understanding have allowed us to apply XAFS spectroscopy to characterize plutonium and other actinide species in a wide variety of chemical environments ranging from contaminated soils (see ARQ 1st Quarter, 2002) to process solutions used in our weapons production mission.

Unusual oxidation states—spectroelectrochemistry

It is difficult to study the unusual oxidation state (VII) at a synchrotron facility due to the length of time between sample preparation at Los Alamos and the actual measurement of its spectrum at a synchrotron facility a thousand miles away. To overcome this obstacle, we developed an electrochemical cell wherein we could prepare Np(VII) and Pu(VII) in situ at the beam line. (For a discussion of related structural studies of Np(VII), see the article on page 15.)

In alkaline solution, Np(VI) exists as a dioxo ion, while Np(VII) displays a tetraoxo unit. These changes in molecular geometry alter the spectral shape of the XANES, which shows two distinct peaks of comparable amplitude for the tetraoxo species instead of the single primary peak and shoulder characteristic of the dioxo structure. A 0.8 eV shift is observed in the edge between Np(VI) and (VII) complexes, consistent with the higher charge of the latter.

The research on aqueous complexes was supported by a Laboratory Directed Research and Development (LDRD) project administered by the Glenn T. Seaborg Institute at Los Alamos National Laboratory. The alkaline chemistry of Np(VII) is supported by the DOE Office of Basic Energy Sciences. XAFS experiments were performed at the Stanford Synchrotron Radiation Laboratory, which is supported by the DOE Office of Basic Energy Sciences.

Transuranics away from home

When Los Alamos programs call for performing experiments with transuranics at a synchrotron x-ray source, how do you do it?

There are only three light sources in the United States: Stanford Synchrotron Light Source, Argonne National Laboratory, and Brookhaven National Laboratory. Less than 1 ppm of plutonium in a 200-mg Rocky Flats concrete sample may be close to an exempt quantity, but Pu-238-spiked alloys or Hanford tank sludges with contact doses of 20 mrem/hr per hour begin to approach the limits for these nonnuclear facilities. And when the sample is a salt in a beryllia holder that is supposed to be melted at 800 °C or an electrochemical cell, then handling even a few milligrams of plutonium becomes a problem.

The answer to this question is to temporarily construct a piece of equipment like that used in Los Alamos' Plutonium Facility (PF-4) at the experimental site.

By working with personnel from Los Alamos' Health Physics Operations Group—integrated safety management long before the phrase was in common use—sample holders are designed, fabricated, tested, loaded, and shipped to the synchrotron, where both the transfer (samples can never be enclosed in less than three layers of containment at any time) and experimental areas have been outfitted with controlled, HEPA-filtered ventilation, continuous air monitors, and other equipment far less common at the light sources than it is here.

While Los Alamos radiological control technicians place samples in tertiary containers and mount them in the diffractometer or on the XAFS sample positioner and monitor the operations, the scientists on the team heat, cool, and electrolyze the samples and perform the actual measurements according to the 24/7 synchrotron schedule.

Although many measurements on transuranics had already been performed at synchrotrons—including many by Los Alamos—prior to the initiation of this program, this was nevertheless the first time that a long-term program of this type was proposed involving many different types of materials and conditions on a continuous basis, and just as the awareness of safety concerns began to be heightened. Conceived in 1991,

during the Tiger Team era, the first experiments at the Stanford Synchrotron Light Source were performed in July 1993 after an approval process that took almost two years.

Since that first 10-day run, scientists, technicians, and students from Los Alamos and many other institutions—including Argonne, Pacific Northwest and Oak Ridge National Laboratories; Great Britain's Atomic Weapons Establishment (AWE) France's Centre de Valduc; the Australian Nuclear Science and Technology Organization; the Institute of Transuranium Elements (ITU), Karlsruhe, Germany; the Paul Scherrer Institute; Rocky Flats; and a number of both foreign and U.S. universities—have collaborated in XAFS and x-ray-scattering measurements on transuranic-containing samples that require the unique properties of synchrotron radiation. These measurements provide results for programs concerned with weapons materials, nuclear fuels, environmental restoration, waste storage, separations chemistry, and other aspects of both basic and applied actinide chemistry and materials science.

Since this pioneering step by Los Alamos, many other groups have duplicated this feat, and measurements on transuranic samples have become so common that most light sources are now being equipped with dedicated facilities for radioactive samples.

And when we're done, we break it down, put it away until the next run, and return home to catch up on our sleep and analyze the data.

To safely study transuranics at the Stanford Synchrotron Light Source, researchers had to outfit the experimental area with controlled, filtered ventilation and continuous air monitors.



An aerial view of the Stanford Synchrotron Light Source.

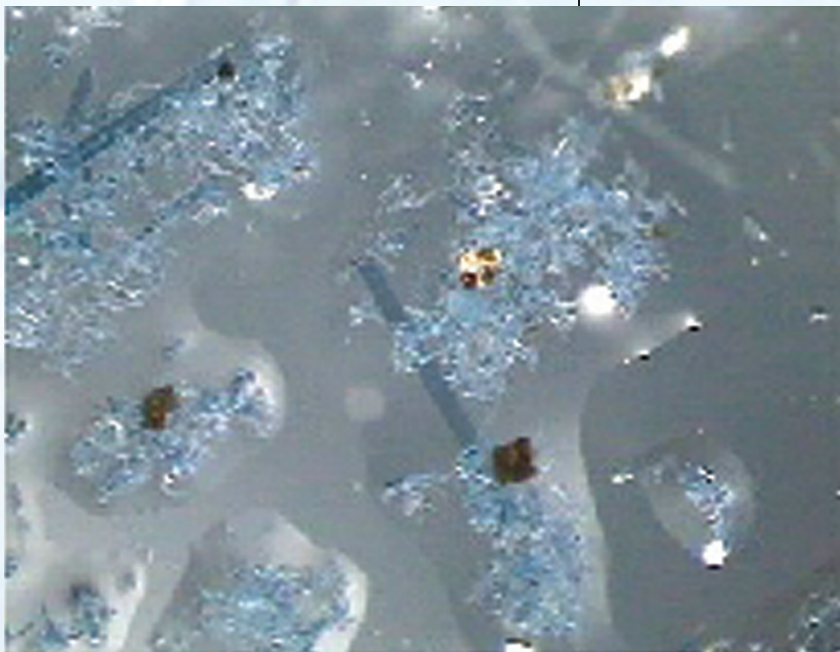
Unraveling the coordination chemistry will improve plutonium separation by precipitation processes

Structural characterization of compounds targeted in plutonium separation for the past 50 years

Since the early days of its discovery, the chemical separation and purification of plutonium has been directly correlated with its applications in weapons and nuclear fuel technologies. However, large-scale processing schemes were often dictated by historically required chemical conditions that were found to be the most convenient for precipitation, ion exchange, or solvent extraction. The pragmatic focus on developing a separation scheme outweighed the need for a more fundamental understanding of the technical basis for plutonium separation.

In more modern times, changing regulatory requirements for lower levels of contaminants in waste waters requires process optimization that, without a fundamental understanding of how the process works, will likely not be achieved. Examples are the precipitation of plutonium oxalate ($C_2O_4^{2-}$) and iodate (IO_3^-) compounds, which were recognized early on as excellent candidates for plutonium separation owing to their remarkably low solubility in slightly acidic solutions.

Oxalate forms strong complexes with the lower oxidation states, Pu(III) and (IV), whereas iodate can effectively precipitate Pu(III), (IV), and (VI). In fact, the use of oxalate to separate plutonium from solution has long been implemented into plutonium purification and waste-treatment processes, while plutonium iodate precipitation has been used less abundantly for analytical purposes. Despite the fact that oxalate and iodate compounds have been applied for about 50 years in large-scale separations, the nature and composition of the actual precipitates are still under debate. Unraveling the uncertainties in the chemistry of these compounds is necessary to improve and optimize the precipitation processes currently used.



Blue Pu(III) oxalate crystals.

This article was contributed by Los Alamos researchers Wolfgang Runde and Brian L. Scott of the Chemistry Division; and Amanda C. Bean, Kent Abney, and Paul H. Smith of the Nuclear Materials Technology Division.

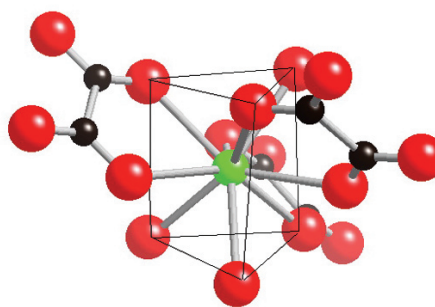
The solid plutonium oxalate system is dominated by two hydrates (crystals incorporating water molecules into their structures), $\text{Pu}_2(\text{C}_2\text{O}_4)_3 \cdot 10\text{H}_2\text{O}$ and $\text{Pu}(\text{C}_2\text{O}_4)_2 \cdot 6\text{H}_2\text{O}$, for which only powder x-ray diffraction data have been reported. Several different hydrates are suggested to exist at different temperatures, without strong experimental evidence regarding how the water molecules are actually bound within the respective crystals.

To gain better insight into the oxalates, we obtained single crystals of blue Pu(III) oxalate by slowly reducing Pu(IV) oxalate in 1 M HCl acid at ambient temperature. The x-ray diffraction analysis revealed this compound to be the hydrated Pu(III) oxalate of formula $\text{Pu}_2(\text{C}_2\text{O}_4)_3(\text{H}_2\text{O})_3 \cdot 3\text{H}_2\text{O}$. (We write the formula this way to indicate that three H_2O molecules are directly bound to each Pu atom, while three H_2O molecules are incorporated in the crystalline lattice.)

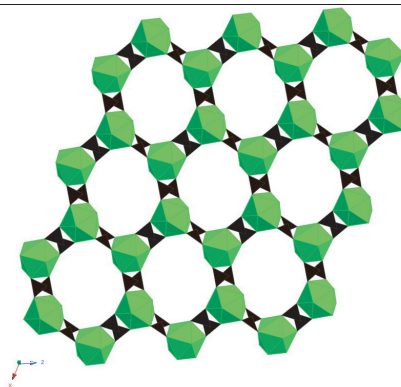
The two-dimensional compound consists of $[\text{PuO}_9]$ polyhedra that are linked by $[\text{C}_2\text{O}_4]$ groups and a network of interstitial water molecules. The plutonium atom is coordinated to six oxygen atoms from three bidentate oxalate ligands and three oxygen atoms from coordinated waters in a distorted tricapped prismatic geometry. In this geometry, six oxygen atoms form the vertices of a trigonal antiprism and each of the three faces is capped by water. The Pu–O distances range between 2.48 Å and 2.57 Å.

In the complex mixtures of actual plutonium process streams and the presence of high concentrations of pyrochemical salt waste such as CaCl_2 or Na/KCl it is expected

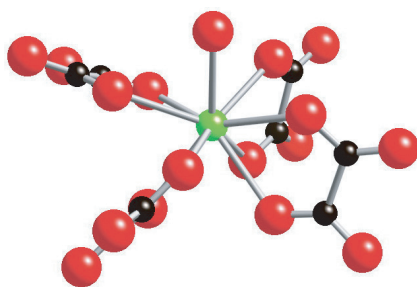
that the binary Pu oxalates incorporate cations (Ca^{2+} , Na^+ , or K^+ ions) in exchange for lattice waters. This exchange would increase the distance between the plutonium oxalate layers as has been observed in many-layered mineral phases. In the presence of K^+ cations and under



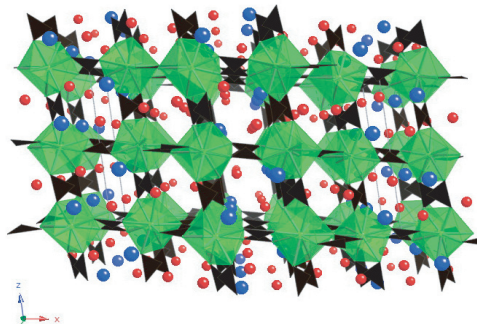
Ball and stick illustration of the $\text{Pu}(\text{C}_2\text{O}_4)_3(\text{H}_2\text{O})_3^{3-}$ unit in the solid Pu(III) oxalate $\text{Pu}_2(\text{C}_2\text{O}_4)_3(\text{H}_2\text{O})_6 \cdot 3\text{H}_2\text{O}$. The dark lines represent the trigonal prism with the Pu atom (green) in the center, which is coordinated to nine O atoms (red). The prism is capped by three O atoms contributed from three oxalate ($\text{C}_2\text{O}_4^{2-}$) groups. C atom (black).



Crystal packing in $\text{Pu}_2(\text{C}_2\text{O}_4)_3(\text{H}_2\text{O})_6 \cdot 3\text{H}_2\text{O}$ viewed down the crystallographic b axis. The two-dimensional structure contains layers that orient themselves in the ac plane. The PuO_9 units are represented as green polyhedra; the planar oxalate groups are black.



Arrangement of the oxalate ligands in the $\text{Pu}(\text{C}_2\text{O}_4)_4(\text{H}_2\text{O})_5^{5-}$ units that build up the Pu(IV) oxalate, $\text{KPu}(\text{C}_2\text{O}_4)_2(\text{H}_2\text{O}) \cdot 2\text{H}_2\text{O}$. The nine-coordinate Pu atom (green) is surrounded by eight O atoms (red) from four oxalate ligands and one water molecule. C atom (black).



View of the three-dimensional structure of the Pu(IV) oxalate $\text{KPu}(\text{C}_2\text{O}_4)_2(\text{H}_2\text{O}) \cdot 2\text{H}_2\text{O}$ along the ac plane. Water molecules (red) and K atoms (purple) are aligned down the b axis. The PuO_9 units are represented as green polyhedra; the planar oxalate groups are black.

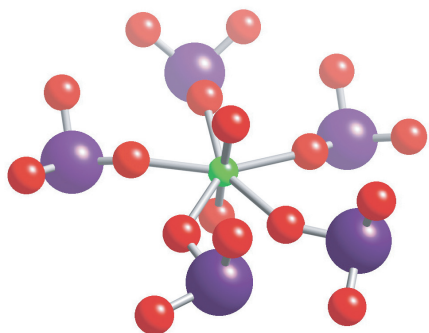
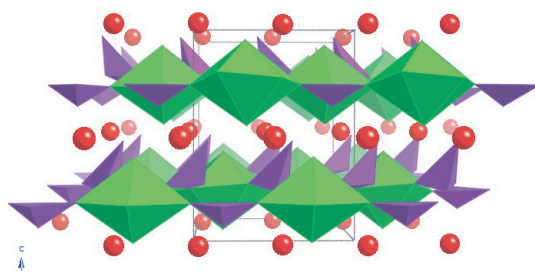


Illustration of the $\text{PuO}_2(\text{IO}_3)_5^{3-}$ building block in the Pu(VI) iodate $\text{PuO}_2(\text{IO}_3)_2 \cdot \text{H}_2\text{O}$. The Pu atom (green) is coordinated in a pentagonal bipyramidal geometry to five iodate anions, IO_3^- (I = purple, O = red) and to two O atoms within the characteristic linear plutonyl, $[\text{O}=\text{Pu}=\text{O}]^{2+}$, moiety.



Crystal packing in $\text{PuO}_2(\text{IO}_3)_2 \cdot \text{H}_2\text{O}$. The two-dimensional solid (viewed down the c axis) contains infinite staggered Pu(VI) iodate layers that are separated by water molecules. The PuO_7 units are represented as green polyhedra; the trigonal iodate groups are purple. O atoms from lattice H_2O molecules are red.

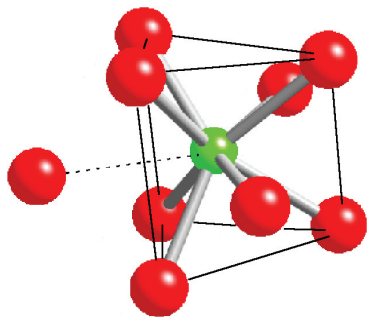
chelating oxalate ($\text{Pu}-\text{O} = 2.48\text{--}2.54 \text{ \AA}$) ligands are arranged around the plutonium atom while one hydroxide ligand ($\text{Pu}-\text{OH} = 2.48 \text{ \AA}$) lies above the plutonium atom. This coordination geometry is similar to that found for the limiting complex of trivalent neodymium in carbonate solution, $\text{Nd}(\text{CO}_3)_4(\text{H}_2\text{O})^{5-}$. It is very likely that $\text{Pu}(\text{C}_2\text{O}_4)_4(\text{OH})^{5-}$ is the limiting solution complex at high oxalate concentrations and assumes very similar coordination geometry as found in the extended structure of $\text{KPu}(\text{C}_2\text{O}_4)_2\text{OH} \cdot 2\text{H}_2\text{O}$.

hydrothermal conditions at 180°C , green crystalline needles of the ternary Pu(IV) oxalate, $\text{KPu}(\text{C}_2\text{O}_4)_2\text{OH} \cdot 2\text{H}_2\text{O}$, were obtained.

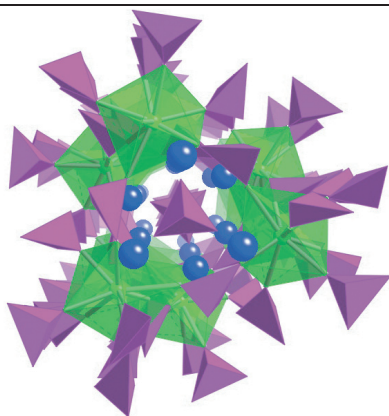
Surprisingly, this compound consists of a three-dimensional framework built up from oxalate-linked $[\text{PuO}_6]$ polyhedra. Although plutonium again exhibits a coordination number of nine, the local coordination geometry is quite different. Eight oxygen atoms from four

Iodate precipitation was used for oxidation state determination of plutonium in October 1942 when Pu(IV) was precipitated from HNO_3 solutions upon addition of HIO_3 or KIO_3 . The calculated molecular weight did not match the suggested formula, $\text{Pu}(\text{IO}_3)_4$, indicating the possible presence of KIO_3 or HIO_3 in the solid or even the presence of other plutonium oxidation states. Due to the oxidizing nature of iodate, synthesizing a crystalline Pu(III) or (IV) iodate has proved an intractable task, raising some doubt as to the validity of a Pu(IV) iodate precipitate. The use of KIO_4 , I_2O_5 , or H_5IO_6 ($E^\circ(\text{IO}_4^-/\text{IO}_3^-) = 1.65 \text{ V}$) led to the complete oxidation of lower plutonium oxidation states to Pu(VI) (i.e., $E^\circ(\text{Pu}^{4+}/\text{PuO}_2^{2+}) = 0.98 \text{ V}$) and the crystallization of a Pu(VI) iodate of formula $\text{PuO}_2(\text{IO}_3)_2 \cdot \text{H}_2\text{O}$.

The binary plutonyl(VI) iodate, $\text{PuO}_2(\text{IO}_3)_2 \cdot \text{H}_2\text{O}$, is unique in its structure and displays previously unknown actinyl-iodate coordination. This plutonyl compound is isostructural with that of $\text{NpO}_2(\text{IO}_3)_2 \cdot \text{H}_2\text{O}$ and consists of infinite staggered layers of $\text{PuO}_2(\text{IO}_3)_2$ with water molecules arranged between the layers. The layers are made up of pentagonal bipyramidal $[\text{PuO}_7]$ polyhedra that are connected by bridging pyramidal IO_3 units.



Coordination environment of Am(III) (green) in the pseudo-tricapped trigonal prismatic coordination in $\text{K}_3\text{Am}_3(\text{IO}_3)_{12} \cdot \text{HIO}_3$. All oxygen atoms (red) originate from eight iodate (IO_3^-) anions, which link the Am polyhedra in a three-dimensional framework. The longer bond between the Am center and the O atom (dashed line) from the neutral HIO_3 molecule completes the ninefold coordination of the Am atom.



Crystal packing in $\text{K}_3\text{Am}_3(\text{IO}_3)_{12} \cdot \text{HIO}_3$. Views of the K (blue)-lined channels formed along the c axis, which are built up from alternating $[\text{AmO}_6]$ polyhedra (green) and iodate (purple) ligands with the neutral HIO_3 (purple) molecules staggered in the center of the channel.

Axial Pu=O bond lengths are 1.75 Å, characteristic for PuO₂²⁺, and equatorial Pu–O distances range between 2.33 and 2.42 Å. Two crystallographically unique iodate anions, IO₃⁻, connect the plutonium atoms. The [I(1)O₃] groups join two plutonium atoms through bridging oxygen atoms, leaving one oxygen atom terminal; in contrast, the other iodate group, [I(2)O₃], coordinates three plutonyl units. This coordination has only been observed previously in the trivalent lanthanide iodate compounds.

To investigate the formation and coordination chemistry of Pu(III) iodates, the chemically analogous Am(III) was used because Am remains stable in its +3 oxidation state even in the presence of any of the iodate sources mentioned ($E^\circ(\text{Am}^{3+}/\text{AmO}_2^{2+}) = 1.69 \text{ V}$). Pink crystals were successfully synthesized by reacting ²⁴³Am(III) in 3 M HCl acid at 180 °C with KIO₄ solutions. X-ray diffraction analysis revealed the compound to be K₃Am₃(IO₃)₁₂·HIO₃, a three-dimensional framework of [AmO₈] units bridged by corner-sharing [IO₃] pyramids. Eight oxygen atoms from eight iodate groups with Am–O distances between 2.42(3) and 2.60(3) Å form a distorted bicapped trigonal prismatic coordination polyhedron.

The most interesting aspect of this compound lies within the microporous channel framework. Three [AmO₈] and three [IO₃] groups form irregular hexagonal channels that are approximately 4.6 Å in diameter. Neutral HIO₃ molecules are staggered in the center of these channels and potassium cations line the cavity with close contacts to the HIO₃ molecule (K–O = 2.40(4) Å). The neutral HIO₃ molecules are anchored in the cavity center through a weak interaction between the oxygen atoms of the HIO₃ molecules and the americium atoms with a longer Am–O distance of 2.93(4) Å.

Although this is the first architecture of its kind among the *f*-element iodates, this structure suggests the possibility of the synthesis of new microporous lanthanide iodates with unique selectivity properties for ion-exchange, catalysis, and photochemical processes. It still must be shown if other molecules of varying size and shape can replace the trapped neutral molecules and if the replacement of potassium cations along the channel exterior will affect the retention strength of the trapped molecules.

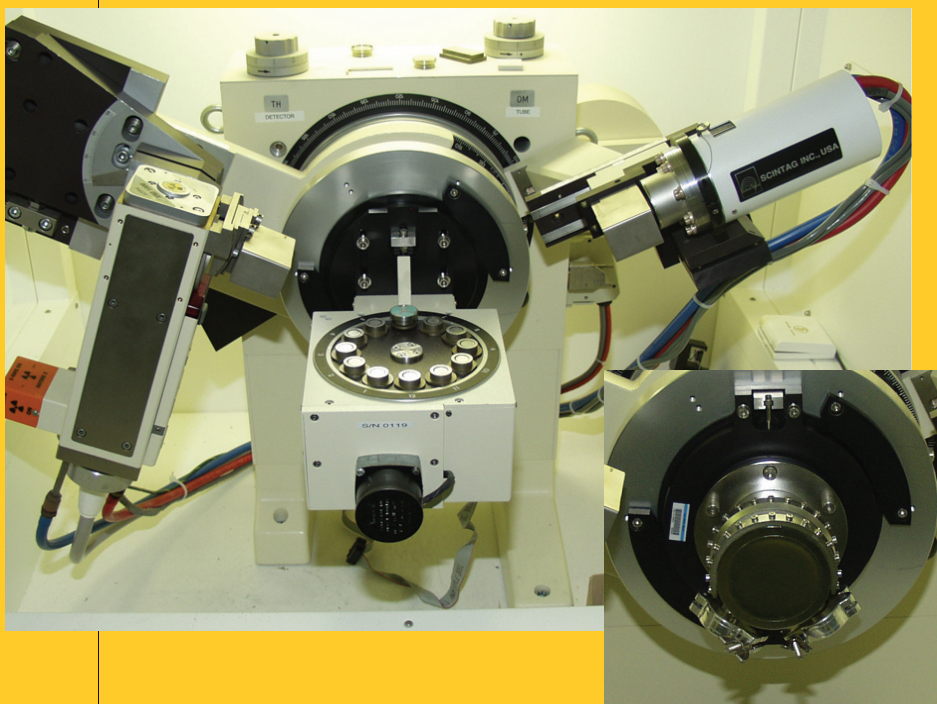
From an academic perspective, structural characterization of transuranium complexes remains rare, and only about a dozen single crystal structures of americium compounds are known. As demonstrated in K₃Am₃(IO₃)₁₂·HIO₃, the coordination chemistry of americium may vary from its chemically analogous lanthanides and offers new insight into differences in bonding of 4*f* and 5*f* elements.

After more than 50 years of technological application of oxalate and iodate compounds, highly crystalline plutonium compounds have now been prepared using hydrothermal synthesis techniques, which has allowed for determination of their structural nature by x-ray diffraction. Chemical synthesis under hydrothermal conditions has proven to be a valuable method for targeting actinide compounds previously only known as amorphous or microcrystalline materials. Chemical conditions that mimic those used for large-scale plutonium separation and purification are used to trigger crystallization under process conditions, and the resulting solid precipitates can subsequently be structurally characterized.

This work was supported by the Glenn T. Seaborg Institute Summer Student fellowship program and the Pu Stabilization and Scrap Recovery Program, under the direction of project leader Paul H. Smith.

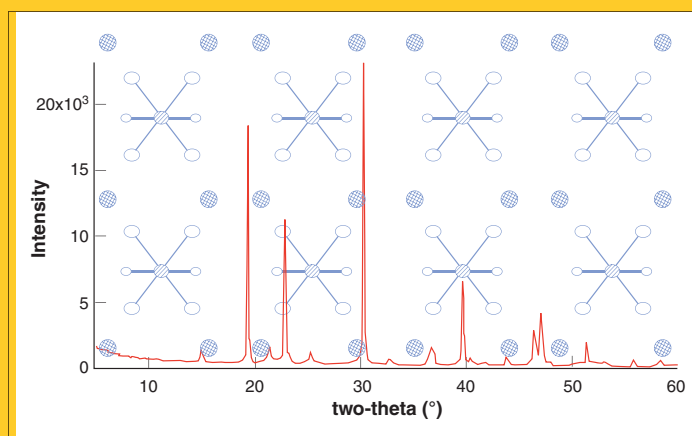
Powder x-ray diffraction

The powder diffraction capability in Los Alamos' Chemistry Division has two diffractometers, which are capable of running a wide variety of samples containing radioactive isotopes. This experimental technique can be used for phase identification of polycrystalline samples. In addition, a new capability is being developed to determine full crystal structures from high-quality polycrystalline samples. Thorium- and uranium-containing samples can be run with a polymeric containment procedure on a 12-position autosampling attachment. Transuranic samples can be run in an airtight environmental chamber, which protects workers and the environment from exposure.



A 12-position autosampler is attached to this x-ray powder diffractometer. The round green disk in the center of the photo is a sample in position for diffraction. The diffractometer can also be fitted with an airtight environmental chamber (inset). X-rays enter and exit through a beryllium window at the top of the chamber. The environmental chamber can be removed and loaded in a glovebox or hood.

The plot of an x-ray diffraction pattern of polycrystalline $Cs_2UO_2Cl_4$ is shown in red. The molecular structure corresponding to the diffraction pattern is depicted in the background. Marianne Wilkerson of Los Alamos' Chemistry Division synthesized the sample.



Photos by
Josh Smith, C-OPS

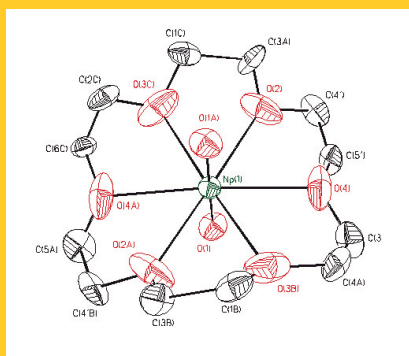
Single-crystal x-ray diffraction

The single-crystal x-ray diffraction capability in Los Alamos' Chemistry Division is a world leader in crystal structure determination of small molecules containing actinide elements. A crystal structure is determined when a crystal is placed in an x-ray beam and the diffraction pattern is measured and analyzed, resulting in a three-dimensional picture of the

molecules comprising the crystal. Researchers have determined 41 transuranic-containing structures in the past 9 years, including plutonium, neptunium, americium, and curium. In addition, more than 300 thorium- and uranium-containing crystal structures have been determined. These structures build on the results of Los Alamos scientist William Zachariasen, who in the 1950s and 1960s determined more than 180 actinide structures of extended solids and alloys. These molecular structures are the foundation for understanding materials and molecular properties and have appeared in scores of papers, including a recent issue of *Nature* (Nov. 21, 2002) and the cover of the *International Edition of Angewandte Chemie* (1997).



To mitigate the associated health hazards of working with transuranic elements, researchers have developed a triple-containment technique for the crystals used in these experiments. The crystal is first coated in epoxy and placed on a glass fiber (left), the crystal and fiber are then placed in a quartz capillary and sealed (middle), and the capillary is coated with acrylic nail polish (right). The acrylic coating keeps the capillary and contents in place in the event of breakage.



The molecular structure of $\text{NpO}_2(18\text{-crown-6})^+$.



Crystallographer Brian Scott of the Chemistry Division adjusts a crystal on the single-crystal diffractometer.



This close-up of a broken capillary containing a crystal shows how the triple-containment technique maintains the integrity of the sample and prevents sample loss in the event of breakage.

Photos by
Josh Smith, C-OPS

Room-temperature ionic liquids

Unusual solvent system shows potential to revolutionize separation and purification technologies

This article was contributed by Los Alamos researchers Warren J. Oldham of the Chemistry Division and Michael E. Stoll and David A. Costa of the Nuclear Materials Technology Division.

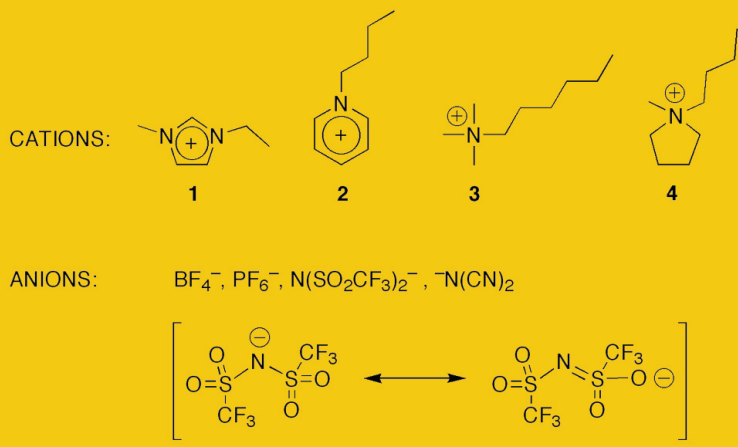
Room-temperature ionic liquids (RTILs) represent an intriguing and highly unusual solvent system in which to carry out basic research and develop advanced separation and purification technologies for the actinide elements. The ionic liquids themselves are the subject of intense worldwide interest, as much for their curious properties as for their potential in revolutionizing chemical synthesis, catalysis, separations, and electrochemistry.

Part of the optimism surrounding ionic liquids rests on their improved safety characteristics as compared to volatile organic solvents and their ability to solubilize both nonpolar organic solutes as well as highly charged inorganic ions. In many cases ionic liquids combine the solvating properties of polar solvents such as water with those of nonpolar organic solvents such as benzene. The ionic liquids are characterized as having negligible vapor pressure, thereby eliminating health effects through airborne exposure, and significantly reducing flammability hazards compared to traditional organic solvents. Additionally, these solvent systems offer a novel chemical environment that may uniquely influence the course of chemical reactions as compared to traditional molecular solvents.

By way of definition, the ionic liquids used in our work are low-melting organic salts, distinct from other classes of solvents in that they are composed of separate and discrete organic cations and weakly coordinating anions. These solvents are nonproton donating and are not related to the more familiar, self-ionizing solvents such as water ($2 \text{H}_2\text{O} = \text{H}_3\text{O}^+ + \text{OH}^-$; ionic product = 10^{-14}), anhydrous hydrofluoric acid, or the various "super acids."

In many respects, RTILs are most closely related to classical molten salts. In theory, some 10 trillion different cation/anion combinations can be used

Classical inorganic salts consist of infinite three-dimensional arrays of close packed spherical ions and are characteristically brittle solids with high melting points (for example, the melting point of NaCl is 801 °C). Low-melting ionic liquids are obtained through two molecular design principles. First, coulombic interactions are minimized by diffusing charge over several atoms in a molecule. In the case of ionic liquid cations, the 1,3-dialkylimidazolium unit (1) is a common example that spreads the positive charge over the five atoms of the heterocyclic ring. Weakly coordinating anions delocalize charge through induction to highly electronegative fluorine atoms or by resonance as shown explicitly for the $^{-}\text{N}(\text{SO}_2\text{CF}_3)_2$ anion. More-complex and higher molecular weight cations and anions have also been explored, but the greater number of intermolecular contacts serve to raise melting points and increase the viscosity in such systems. For convenience in routine use as solvents, lower molecular weight constituents are preferred. The second design principle in ionic liquid synthesis is molecular asymmetry. All things being equal, low-symmetry cations and anions reduce packing efficiency in the crystalline state and lower melting points. A dramatic example is provided by the comparison of the PF_6^{-} and $^{-}\text{N}(\text{SO}_2\text{CF}_3)_2$ salts of cation 1, which melt at 58 °C and -3 °C, respectively.



to produce binary ionic liquid systems. This flexibility affords the potential to tune or “design” the ionic liquid solvent for specific applications. In practice, the requirements for low viscosity and ease (low cost) of synthesis have limited the choice of cation to relatively low molecular weight organic salts complemented by weakly coordinating inorganic anions.

Recent work has employed imidazolium or quaternary ammonium salts of the bis(trifluoromethanesulfonyl)imide anion ($\text{N}(\text{SO}_2\text{CF}_3)_2$ abbreviated as NTf_2) because they are easily prepared, chemically and thermally robust, and yield low-viscosity/high-conductivity anhydrous fluids. Because of their good solubilization characteristics and wide electrochemical window, these solvents are an ideal choice for studying the basic electrochemical behavior of soluble actinide complexes with an eye toward developing redox-based separations technology. Our research has shown that high-quality electrochemical data can be obtained in these ionic liquids on par with what is possible in conventional electrochemical solution media.

We have also focused on understanding the solvent (i.e., coordinating) properties of these ionic liquids. Using a combination of Lewis-acid- and Lewis-base-specific solvatochromic probe molecules that change color as a function of chemical environment, we find that the Lewis-acid properties of the ionic liquids depend on the organic cation and are generally comparable to aliphatic alcohols such as ethanol or butanol. The Lewis basicity, determined by the NTf_2 anion, lies between very weakly coordinating solvents such as nitromethane and more-coordinating solvents such as THF.

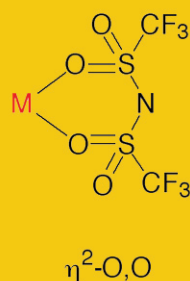
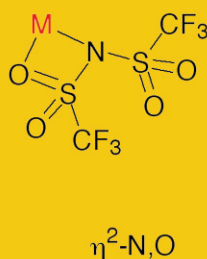
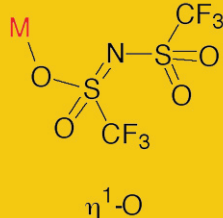
The discovery that ionic liquids are simultaneously weakly Lewis acidic and weakly Lewis basic is consistent with the fact that these salts are liquids at room temperature. This observation indicates that they are characterized by very low lattice energies determined by weak coulombic interactions between the cations and anions.

Salts composed of stronger Lewis acids/bases are more likely to exist as solids at room temperature. These studies highlight the differences between ionic liquids and classical high-temperature molten salts. The solvating properties of the ionic liquids more closely resemble weakly coordinating organic solvents, with the distinct difference that they are highly conductive and the ionic constituents can move independently to stabilize charged solutes.

A comparison in the behavior of two simple U(IV) chloride complexes illustrates the unique chemistry observed in ionic liquids as compared with traditional molecular solvents. Tetrabutylammonium salts of U(IV) hexachloride, $[\text{NBu}_4]_2\text{UCl}_6$, readily dissolve in the ionic liquid solvent to give pale blue solutions with a solubility limit of about 0.1 M. Probing the solutions via cyclic voltammetry experiments indicates that reduction of the U(IV) complex to U(III) or oxidation to U(V) is chemically reversible and that the six chloride ligands remain tightly bound to the metal center throughout these electron-transfer reactions.

In a similar fashion, the coordinatively unsaturated uranium tetrachloride complex, UCl_4 , also dissolves with gentle warming to give deep-green solutions with a solubility limit of about 0.4 M at room temperature. It is known that UCl_4 dissolves in coordinating organic solvents such as acetonitrile or THF to give eight coordinate adducts of the form, $\text{UCl}_4(\text{L})_4$ (L = donor solvent). In contrast, we have discovered that when dissolved in the ionic liquid, UCl_4 undergoes a facile chloride redistribution reaction to give mixtures of $[\text{UCl}_6]^{-2}$ and additional species stabilized by five or fewer chloride ions. Well-formed x-ray-quality single crystals of $[\text{cation}]_2\text{UCl}_6$ readily separate from these solutions, where the cation identified in each case is derived from the particular ionic liquid used in the experiment.

IONIC LIQUIDS



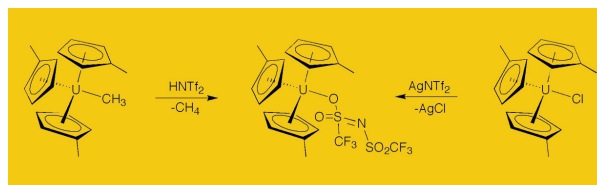
The NTf_2^- anion provides a range of coordination modes to accommodate the particular electronic and steric preferences of a metal ion. Softer metals, represented by low-valent transition metal complexes, display coordination to the nitrogen atom as $\eta^1\text{-N}$ or $\eta^2\text{-N,O}$. High-valent transition metal and actinide complexes prefer oxygen coordination as $\eta^1\text{-O}$ or $\eta^2\text{-O,O}$, depending on the availability of one or two open coordination sites.

Ligand redistribution of this type is surprisingly common in actinide coordination chemistry, driven by the stabilization afforded by maximizing steric saturation. For example, while $\text{UCl}_4(\text{DMSO})_3$ appears to be a reasonable complex, in fact this system exists as a complex salt of the form $[\text{UCl}_2(\text{DMSO})_6][\text{UCl}_6]$ (DMSO = dimethylsulfoxide). In NTf_2^- -based ionic liquid systems, coordinately unsaturated uranium

species are no doubt stabilized by interactions with the anion. We have shown that these interactions are weak by adding two equivalents of chloride ion (as the tetrabutylammonium salt) to yield pure $[\text{UCl}_6]^{2-}$ solutions.

Given the unexpected complexity of the chloride system and the implication that the NTf_2^- anion is playing an active role in the coordination chemistry of unsaturated metal species, we have set out to document the fundamental binding properties of this anion and to help understand how these interactions determine resultant redox properties.

A series of coordinately unsaturated metal species was generated either through the reaction of metal alkyl complexes with HNTf_2 or through reaction of metal halide complexes with AgNTf_2 , as illustrated for the $(\text{C}_5\text{H}_4\text{Me})_3\text{U}$ fragment shown in the following equation.



Single-crystal x-ray diffraction experiments for a number of different metal complexes revealed that four different binding modes were possible for the NTf_2^- anion. The anion can bind in a monodentate fashion either through the nitrogen atom or through one of the sulfonyl oxygen atoms. For less sterically constrained metal species, two different bidentate binding modes were also identified, either via two oxygen atoms from each end of the bis(sulfonyl)imide moiety or via a more acute nitrogen-oxygen interaction. Electronically the NTf_2^- anion behaves as a weakly coordinating anion that donates limited electron density to the metal center.

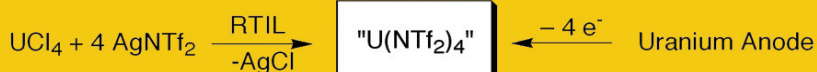
The redox consequences of NTf_2^- ligation are clearly illustrated by comparison of the $4^+/3^+$ redox couples for $(\text{C}_5\text{H}_5)_2\text{TiCl}_2$ and $(\text{C}_5\text{H}_5)_2\text{Ti}(\text{NTf}_2)_2$. While the titanium dichloride system is reversibly reduced at about -1.43 V versus Ag/Ag^+ reference electrode, the $(\text{C}_5\text{H}_5)_2\text{Ti}(\text{NTf}_2)_2$ complex is reduced at -0.49 V, a stabilization of 0.94 V. These are very large effects that suggest the potential to significantly stabilize low-valence metal species in the ionic liquid medium. The possibility of directly electroplating very active actinide metals is also suggested by the stabilization of low-valence complexes. We recognized these observations as an opportunity to directly study the simplest of metal systems by introducing “bare” metal ions into the ionic liquid solvent in the absence of any competing ligands.

In the case of uranium, we found that reaction of UCl_4 with four equivalents of AgNTf_2 or anodic oxidation of a uranium electrode immersed in the ionic liquid solvent produced deep green U(IV) solutions that were identical when characterized by UV/vis spectroscopy.

These results suggest that the U(IV) ion is likely stabilized by ligation to four NTf_2^- anions, each coordinated in a bidentate fashion through the oxygen atoms. Such a binding

mode is reminiscent of well-characterized actinide β -diketonate complexes.

characterization. These solvents do, however, allow facile spectroscopic and electrochemical characterization opportunities for the study of novel actinide coordination chemistry. The study of the actinides in



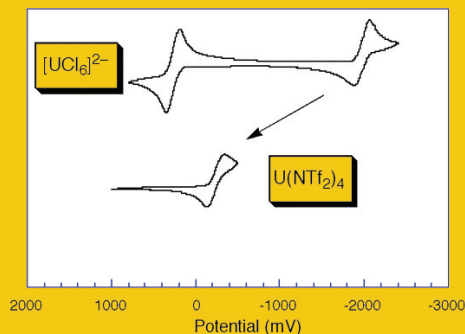
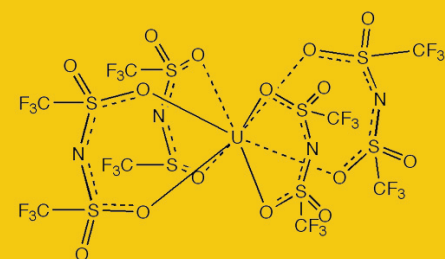
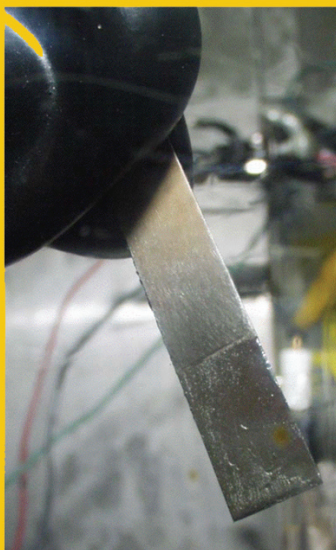
Similar to the titanium complex, the effect of removing the chloride ligands from the U(IV) metal center is profound. In the case of $[\text{UCl}_6]^{2-}$ the $4^+/3^+$ reduction potential is measured at -1.98 V versus Ag/Ag^+ , while for $\text{"U(NTf}_2)_4\text{"}$ this reduction occurs at -0.24 V , a stabilization of 1.74 V . Additionally, despite the extreme electrophilicity (strongly electron-attracting) indicated by this shift in reduction potential, no evidence was found for decomposition of the ionic liquid in the presence of such a potentially reactive U(IV) ion. The behavior of the electrochemically produced U(III) ions at more negative electrode potentials is under active investigation.

The study of actinide elements in ionic liquid solvents presents a number of challenges in the areas of product isolation and structural

ionic liquids is therefore complementary to parallel investigations in aqueous and organic solvents, as well as high-temperature molten salts.

Ultimately, the prospect of preparing new classes of compounds and discovering new reactivity patterns that might be exploited in advanced separations technology guides this work. Given the complementary roles of aqueous/organic solvent extraction, ion exchange chromatography, and high-temperature molten salt electrorefining in current actinide processing and purification practice, we believe that ionic liquids might be used to develop new technologies that combine these disparate tasks into one integrated unit operation with possible advantages in production efficiency, safety, and space requirements.

U(IV) cations can be introduced into the ionic liquid solvent without the complication of additional halide anions by electrochemically dissolving a sacrificial uranium anode in a two-compartment cell. An electrochemically etched uranium anode produced by this process is shown in the photo. Spectroscopic characterization of the resulting green solutions indicate that U(IV) is the dominant oxidation state. The uranium ions are likely to be stabilized by the -NTf_2 anions that compose the ionic liquid and the proposed structure of $\text{U(NTf}_2)_4$ is indicated in the top right. A comparison of the electrochemical behavior of $[\text{UCl}_6]^{2-}$ and $\text{U(NTf}_2)_4$ is shown in the lower right. The $4^+/3^+$ reduction potential is increased by 1.74 V upon elimination of the six chloride anions from the metal's coordination sphere.



This article was contributed by Los Alamos researcher F. Jeffrey Martin, of the Nuclear Nonproliferation Division.



Los Alamos played key role in bilateral effort **Russian secure storage facility commissioned**

After an extensive twelve-year bilateral effort, the Russian Fissile Material Storage Facility (RFMSF) located at Mayak was commissioned by Minatom Dec. 10, 2003. The RFMSF is a United States-sponsored secure storage facility built to hold fissile material derived from dismantled Russian nuclear weapons. The complex is about the size of the Pentagon's footprint and will be the largest, most secure such facility in Russia. Russia plans to load 24 metric tons of weapons useable plutonium, but it has a capacity of 100 metric tons, should additional excess material be declared.

This \$412M project is one of the most successful Nunn-Lugar programs. It is expected to become fully operational and begin receiving plutonium sometime in 2004, after all integrated systems testing and personnel training have been completed, and security measures have been activated. Completion of this facility is considered to be the largest single step toward safeguarding the international stockpile of weapons useable material and contribution to international nonproliferation efforts.

Los Alamos played a key and continuous role from the project's inception to its completion with more than 190 staff participating. Over the history of the RFMSF project, Los Alamos had three broad roles: to provide advanced nuclear material facility technology to modernize the Russians' approach to nuclear safety, and fissile material control, and accountability; to technically evaluate the facility design, construction, and pre-operational state to confirm the facility will meet its mission and provide safe, secure, and ecologically sound storage of fissile material; and to provide and evaluate state-of-the-art technology for the Defense Threat Reduction Agency to support facility transparency measures for future verification activities during operations.

The Laboratory's achievements over the life of the project were numerous, despite many obstacles. Within this challenging environment Los Alamos provided the Russians extensive access to Western methods and technology to perform their own nuclear safety analysis that would stand up to international scrutiny. Lab researchers reviewed the thermal design of the RFMSF and thermal environment of the plutonium and led a large bilateral thermal program of analysis and full-scale experiments that confirmed a substantial thermal margin in the design. This effort determined the plutonium capacity could be increased from 33 to 100 metric tons, sufficient to hold all of Russia's excess plutonium for the foreseeable future.

Los Alamos also completed a technically comprehensive safety and ecological analysis and evaluation that confirmed the safety adequacy of the facility per U.S. and International Atomic Energy Agency (IAEA) safety standards; evaluated the adequacy of the facility measures for fissile material control, physical protection and accountability, and facility security; and provided the technical backbone of the U.S. transparency program by conducting an extensive radiation measurement campaign for a database for nondestructive fissile material mass measurements and providing expert support to the U.S. transparency negotiating team.

These many efforts culminated in the successful completion of the facility and confirmation that it is capable of making the world a safer place.

Actinide Research Quarterly
is produced by Los Alamos
National Laboratory

About the Quarterly

ACTINIDE RESEARCH QUARTERLY highlights recent achievements and ongoing programs of the Nuclear Materials Technology (NMT) Division. We welcome your suggestions and contributions. ARQ can be read on the World Wide Web at:
<http://www.lanl.gov/orgs/nmt/nmtdo/AQarchive/AQhome/AQhome.html>

Address correspondence to
Actinide Research Quarterly
c/o Meredith Coonley
Mail Stop E500
Los Alamos
National Laboratory
Los Alamos, NM 87545

If you have questions, comments, suggestions, or contributions, please contact the ARQ staff at
arq@lanl.gov.

Phone (505) 667-0392
Fax (505) 665-7895

ARQ Staff

NMT Division Director
Steve Yarbrow

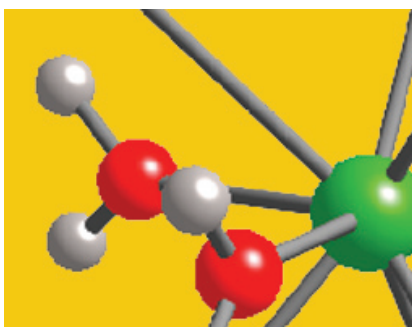
*Scientific Advisors,
Seaborg Institute*
David L. Clark
Gordon D. Jarvinen

Editor
Meredith S. Coonley, IM-1

Designer
Susan L. Carlson, IM-1

Contributing Writers/Editors
Vin LoPresti, IM-1
Garth Giesbrecht, NMT-DO
Ed Lorusso, NMT-3

Printing Coordination
Lupe Archuleta, IM-4



Los Alamos National Laboratory, an affirmative action/equal opportunity employer, is operated by the University of California for the U.S. Department of Energy under contract W-7405-ENG-36. All company names, logos, and products mentioned herein are trademarks of their respective companies. Reference to any specific company or product is not to be construed as an endorsement of said company or product by the Regents of the University of California, the United States Government, the U.S. Department of Energy, nor any of their employees. Los Alamos National Laboratory strongly supports academic freedom and a researcher's right to publish; as an institution, however, the Laboratory does not endorse the viewpoint of a publication or guarantee its technical correctness.

LALP-04-060



